NATIONAL ADVISORY COMMITTEE FOR AERONAUTICS

REPORT No. 777

THE THEORY OF PROPELLERS III—THE SLIPSTREAM CONTRACTION WITH NUMERICAL VALUES FOR TWO-BLADE AND FOUR-BLADE PROPELLERS

By THEODORE THEODORSEN

1944

For sale by the Superintendent of Documents - U. S. Government Printing Office - Washington 25, D. C. - Price 20 cents

AERONAUTIC SYMBOLS

1. FUNDAMENTAL AND DERIVED UNITS

	Symbol	Metric		English	
		Unit	Abbreviation	Unit	Abbreviation
Length	l	meter	m	foot (or mile)	ft (or mi)
Time	t	second	s	second (or hour)	sec (or hr)
Force	F	weight of 1 kilogram	kg	weight of 1 pound	lb
Power	P	horsepower (metric)		horsepower	hp
Speed	V	kilometers per hour	kph	miles per hour	mph
		meters per second	mps	feet per second	fps

2. GENERAL SYMBOLS

W Weight$=mg$

g Standard acceleration of gravity$=9.80665$ m/s^2 or 32.1740 ft/sec^2

m Mass$=\frac{W}{g}$

I Moment of inertia$=mk^2$. (Indicate axis of radius of gyration k by proper subscript.)

μ Coefficient of viscosity

ν Kinematic viscosity

ρ Density (mass per unit volume)

Standard density of dry air, 0.12497 kg-m^{-4}-s^2 at 15° C and 760 mm; or 0.002378 lb-ft^{-4} sec^2

Specific weight of "standard" air, 1.2255 kg/m^3 or 0.07651 lb/cu ft

3. AERODYNAMIC SYMBOLS

S Area

S_w Area of wing

G Gap

b Span

c Chord

A Aspect ratio, $\frac{b^2}{S}$

V True air speed

q Dynamic pressure, $\frac{1}{2}\rho V^2$

L Lift, absolute coefficient $C_L=\frac{L}{qS}$

D Drag, absolute coefficient $C_D=\frac{D}{qS}$

D_0 Profile drag, absolute coefficient $C_{D0}=\frac{D_0}{qS}$

D_i Induced drag, absolute coefficient $C_{Di}=\frac{D_i}{qS}$

D_p Parasite drag, absolute coefficient $C_{Dp}=\frac{D_p}{qS}$

C Cross-wind force, absolute coefficient $C_C=\frac{C}{qS}$

i_w Angle of setting of wings (relative to thrust line)

i_t Angle of stabilizer setting (relative to thrust line)

Q Resultant moment

Ω Resultant angular velocity

R Reynolds number, $\rho\frac{Vl}{\mu}$ where l is a linear dimension (e.g., for an airfoil of 1.0 ft chord, 100 mph, standard pressure at 15° C, the corresponding Reynolds number is 935,400; or for an airfoil of 1.0 m chord, 100 mps, the corresponding Reynolds number is 6,865,000)

α Angle of attack

ϵ Angle of downwash

α_0 Angle of attack, infinite aspect ratio

α_i Angle of attack, induced

α_a Angle of attack, absolute (measured from zero-lift position)

γ Flight-path angle

ERRATUM

NACA REPORT No. 777

THE THEORY OF PROPELLERS
III - THE SLIPSTREAM CONTRACTION WITH NUMERICAL
VALUES FOR TWO-BLADE AND FOUR-BLADE PROPELLERS
By Theodore Theodorsen
1944

Page 18, figure 7(a): The bottom part of the lowest curve in the lower left-hand corner of the figure should be —— - — instead of —— - - ——.

REPORT No. 777

THE THEORY OF PROPELLERS III—THE SLIPSTREAM CONTRACTION WITH NUMERICAL VALUES FOR TWO-BLADE AND FOUR-BLADE PROPELLERS

By THEODORE THEODORSEN
Langley Memorial Aeronautical Laboratory
Langley Field, Va.

National Advisory Committee for Aeronautics

Headquarters, 1500 New Hampshire Avenue NW., Washington 25, D. C.

Created by act of Congress approved March 3, 1915, for the supervision and direction of the scientific study of the problems of flight (U. S. Code, title 49, sec. 241). Its membership was increased to 15 by act approved March 2, 1929. The members are appointed by the President, and serve as such without compensation.

REPORT No. 777

THE THEORY OF PROPELLERS

III—THE SLIPSTREAM CONTRACTION WITH NUMERICAL VALUES FOR TWO-BLADE AND FOUR-BLADE PROPELLERS

By Theodore Theodorsen

SUMMARY

As the conditions of the ultimate wake are of concern both theoretically and practically, the magnitude of the slipstream contraction has been calculated. It will be noted that the contraction in a representative case is of the order of only 1 percent of the propeller diameter. In consequence, all calculations need involve only first-order effects. Curves and tables are given for the contraction coefficient of two-blade and four-blade propellers for various values of the advance ratio; the contraction coefficient is defined as the contraction in the diameter of the wake helix in terms of the wake diameter at infinity. The contour lines of the wake helix are also shown at four values of the advance ratio in comparison with the contour lines for an infinite number of blades.

INTRODUCTION

Since reference is often made to the wake infinitely far behind the propeller, it is desirable to establish certain relationships between the dimensions of the propeller and those of the wake helix at infinity. The present paper considers the relationship of the propeller diameter and the wake diameter, or the problem of the slipstream contraction.

The discussion is restricted to a consideration of first-order effects, that is, to the determination of the contraction per unit of loading for infinitely small loadings only. It will be seen that the contractions are indeed very small, of the order of a few percent of the propeller diameter, and that the high-order terms are therefore not of concern. The interference velocity accordingly is neglected as small compared with the stream velocity. The wake helix lies on a perfect cylinder and the pitch angle is everywhere the same. It is noted that the assumption of zero loading corresponds to that used by Goldstein for a different purpose.

SYMBOLS

R tip radius of propeller

r radius of element of vortex sheet

Δr contraction

Δr_0 total contraction or contraction at $\frac{h}{R}=0$

τ angle between starting point of spiral line and point P

H pitch of spiral

θ angular coordinate on vortex sheet

$h=H\frac{\theta}{2\pi}$

λ advance ratio $\left(\frac{H}{2\pi R}\right)$

x ratio of radius of element to tip radius of vortex sheet (r/R)

v_R radial velocity

V advance velocity of propeller

w rearward displacement velocity of helical vortex surface

$\overline{w}=\frac{w}{V}$

p number of blades

κ mass coefficient

$c_s=2\kappa\overline{w}$

Γ circulation at radius x $\left(\Gamma=\frac{\pi c_s \lambda V R}{\kappa}K(x)\right)$

$K(x)$ circulation function for single rotation $\left(\frac{p\Gamma\omega}{2\pi V w}\right)$

ω angular velocity of propeller, radians per second

y_1 radial velocity at point P due to a doublet element at θ,x except for a constant factor

$$\left(y_1=\frac{[\theta\cos(\theta+\tau)-\sin(\theta+\tau)]\,[1-2x^2+\lambda^2\theta^2+x\cos(\theta+\tau)]}{[1+x^2+\lambda^2\theta^2-2x\cos(\theta+\tau)]^{5/2}}\right)$$

$$y_2=\frac{K(x)}{p}\sum_n y_1 \text{ where } n=0,\ 1,\ 2,\ \ldots\ p-1$$

$$Y_1=\int_0^1 y_2\,dx$$

Y_2 angle of contraction, except for a constant factor $\left(Y_2=\int_\theta^\infty Y_1\,d\theta\right)$

Y_3 contour line of contraction, except for a constant factor $\frac{c_s}{\kappa}\frac{\lambda^3}{4}\left(Y_3=\int_0^\infty Y_2\,d\theta\right)$

$\frac{\Delta r_0}{R}$ total contraction in terms of radius $\left(\frac{c_s}{\kappa}\frac{\lambda^3}{4}Y_3\right)$

$\frac{\Delta r_0}{R}\frac{\kappa}{c_s}$ contraction coefficient $\left(\frac{\lambda^3}{4}Y_3\right)$

$$z_1=\sin\phi\left\{\tan^2\phi\left(x^{-1/2}-x^{1/2}\right)E(k)+2x^{1/2}[F(k)-E(k)]\right\}$$

$$w_1=\left[\left(\frac{2}{k}-k\right)F(k)-\frac{2}{k}E(k)\right]^{x=1}$$

THEORY

The radial velocity is obtained by using the Biot-Savart law and integrating over the entire surface of discontinuity. If Δr_0 is the total contraction, the problem is to determine the ratio $\frac{\Delta r_0}{R}$ for various numbers of blades at several advance ratios. Simple expressions referring to zero loading are used throughout.

The radial inward velocity dv_R' at the point P is calculated. (See figs. 1 and 2.) This velocity results from an element

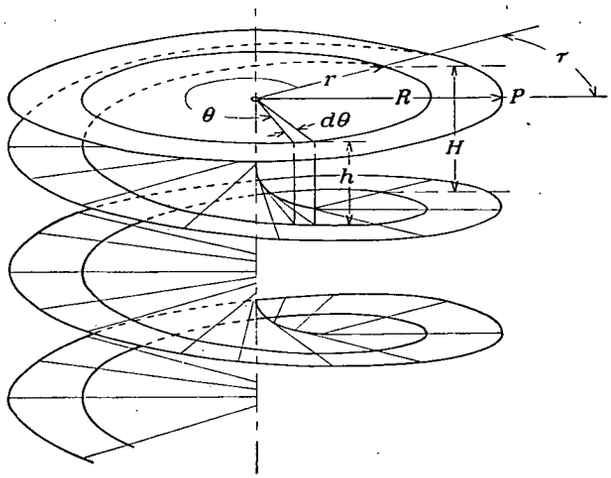

FIGURE 1.—Geometric relationships of wake helix.

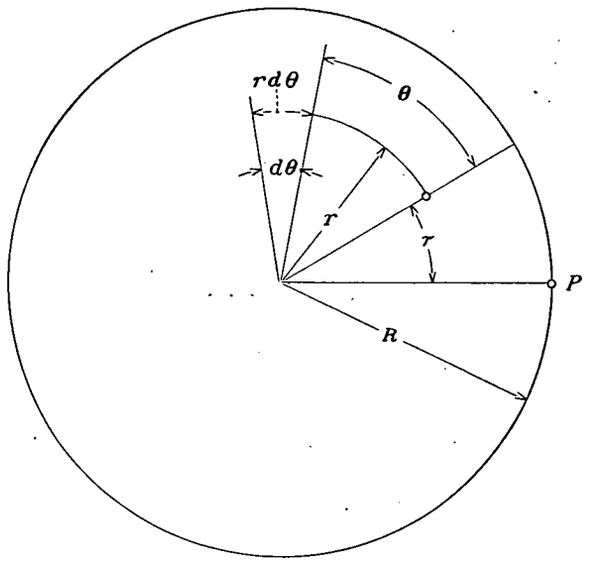

FIGURE 2.—Plan view of wake helix showing geometric relationships.

of circulation $f\,ds$, which is located on a spiral of radius r that starts in a plane perpendicular to the axis and containing the reference point P. The angle between the starting point of the spiral line and the point P is designated τ. The spiral extends below the plane to infinity. If the pitch of this spiral is designated H, the element at a projected angle θ from the starting point of the spiral is then at a distance h below the reference plane where

$$h=H\frac{\theta}{2\pi} \tag{1}$$

By introducing the nondimensional quantities

$$\left.\begin{aligned}\lambda&=\frac{H}{2\pi R}\\ x&=\frac{r}{R}\end{aligned}\right\} \tag{2}$$

in the Biot-Savart law, the following expression is obtained for the radial inward velocity dv_R' due to an element on the wake helix of strength f:

$$dv_R'=\frac{1}{4\pi}\frac{f\,d\theta}{R}\lambda x\frac{\theta\cos(\theta+\tau)-\sin(\theta+\tau)}{[1+x^2+\lambda^2\theta^2-2x\cos(\theta+\tau)]^{3/2}} \tag{3}$$

By differentiating equation (3) with respect to x, the field of a doublet element on the helical vortex sheet is obtained, the doublet element consisting of two neighboring singlet elements each of strength f. Setting $f\,dx$ equal to Γ and dividing through by the stream velocity V gives

$$\frac{dv_R}{V}=-\frac{1}{4\pi}\frac{\Gamma\,d\theta}{RV}\lambda\frac{[\theta\cos(\theta+\tau)-\sin(\theta+\tau)]\,[1-2x^2+\lambda^2\theta^2+x\cos(\theta+\tau)]}{[1+x^2+\lambda^2\theta^2-2x\cos(\theta+\tau)]^{5/2}} \tag{4}$$

where v_R is the radial velocity at the point P.

Equation (4) may be written in the form

$$\frac{dv_R}{V}=-\frac{1}{4\pi}\frac{\Gamma\,d\theta}{RV}\lambda y_1 \tag{5}$$

where

$$y_1=\frac{[\theta\cos(\theta+\tau)-\sin(\theta+\tau)]\,[1-2x^2+\lambda^2\theta^2+x\cos(\theta+\tau)]}{[1+x^2+\lambda^2\theta^2-2x\cos(\theta+\tau)]^{5/2}} \tag{6}$$

The function y_1 is plotted against $\theta+\tau$ for four values of λ and various values of τ and x in figures 3 to 6. With

$$\begin{aligned}\Gamma&=\frac{2\pi Vw}{p\omega}K(x)\\ &=\frac{2\pi V^2\overline{w}}{p\omega}K(x)\\ &=\frac{\pi VR\lambda c_s}{p\kappa}K(x)\end{aligned} \tag{7}$$

where

$$\begin{aligned}c_s&=\frac{2\kappa w}{V}\\ &=2\kappa\overline{w}\end{aligned} \tag{8}$$

substitution in equation (5) gives

$$\frac{dv_R}{V}=-\frac{\lambda^2}{4}\frac{c_s}{\kappa}\frac{K(x)}{p}\,y_1\,d\theta \tag{9}$$

If the point P is at a distance $h=H\frac{\theta}{2\pi}$ below the propeller, integrating equation (9) over the wake yields

$$\frac{v_R}{V}=-\frac{\lambda^2}{4}\frac{c_s}{\kappa}\int_{-\theta}^{\infty}\int_0^1\frac{K(x)}{p}\sum_n y_1\,dx\,d\theta \tag{10}$$

It is noted that, with equally spaced blades, the function

$$\sum_n y_1 \tag{11}$$

is an odd function of θ and

$$\sum_n\int_{-\theta}^{\theta} y_1\,d\theta=0 \tag{12}$$

Equation (10) can therefore be rewritten as

$$\frac{v_R}{V}=-\frac{\lambda^2}{4}\frac{c_s}{\kappa}\int_{\theta}^{\infty}\int_0^1\frac{K(x)}{p}\sum_n y_1\,dx\,d\theta \tag{13}$$

Let

$$\left.\begin{aligned} y_2&=\frac{K(x)}{p}\sum_n y_1\\ Y_1&=\int_0^1 y_2\,dx\\ Y_2&=\int_{\theta}^{\infty} Y_1\,d\theta\end{aligned}\right\} \tag{14}$$

Values of Y_1 and Y_2, multiplied by a constant factor for convenience in plotting, are given in tables I to IV for two-blade and four-blade propellers for which λ and θ take on various values. These functions are plotted against θ in figures 7 and 8.

Equation (13) becomes

$$\frac{v_R}{V}=-\frac{\lambda^2}{4}\frac{c_s}{\kappa}Y_2 \tag{15}$$

Now

$$\frac{v_R}{V}=\frac{dr}{dh}=\frac{d\frac{r}{R}}{d\frac{h}{R}}=\frac{1}{\lambda}\frac{dx}{d\theta} \tag{16}$$

Therefore

$$\frac{dx}{d\theta}=\lambda\frac{v_R}{V}=-\frac{\lambda^3}{4}\frac{c_s}{\kappa}Y_2 \tag{17}$$

whence

$$\frac{\Delta r}{R}=\frac{R_2-R_1}{R}=\frac{1}{R}\int_{R_1}^{R_2}dr=\int_{x_1}^{x_2}dx=-\frac{\lambda^3}{4}\frac{c_s}{\kappa}\int_{\theta_1}^{\theta_2}Y_2\,d\theta \tag{18}$$

If R_2 is the radius at the propeller and R_1 is the ultimate radius of the wake ($\theta_2=0$, $\theta_1=\infty$),

$$\frac{\Delta r_0}{R}=\frac{c_s}{\kappa}\frac{\lambda^3}{4}\int_0^{\infty}Y_2\,d\theta=c_s\frac{\lambda^3}{4\kappa}Y_3 \tag{19}$$

where

$$Y_3=\int_0^{\infty}Y_2\,d\theta$$

Values of Y_3 are given in tables V and VI and are plotted in figure 9 for two-blade and four-blade propellers for which λ and θ take on various values.

After all substitutions are made, the complete multiple integral for the total contraction is obtained as

$$\frac{\Delta r_0}{R}=\frac{c_s}{\kappa}\frac{\lambda^3}{4}\int_0^{\infty}\int_0^{\infty}\int_0^1 K(x)\frac{1}{p}\sum_n y_1(\theta,x)dx\,d\theta\,d\theta$$

(See figs. 10 and 11.)

INFINITE NUMBER OF BLADES

For purposes of comparison, it is useful to obtain the contraction for the case of an infinite number of blades. By resolving the circulation into components parallel to and perpendicular to the axis of the wake, the helical vortices can be replaced by a system of vortices parallel to the axis and another of ring vortices having centers on the axis. Only the ring vortices contribute to the radial velocity.

The field due to a vortex ring of strength f and radius $r=Rx$, located at a distance h below the reference point P, is given by Lamb (reference 1, p. 237). In the notation of the present paper it is

$$\psi_0'=-\frac{fR}{2\pi}x^{1/2}\left[\left(\frac{2}{k}-k\right)F(k)-\frac{2}{k}E(k)\right] \tag{20}$$

where $E(k)$ and $F(k)$ are the complete elliptic integrals and

$$k^2=\frac{4x}{\left(\frac{h}{R}\right)^2+(1+x)^2}$$

As before, a doublet ring is obtained by differentiating equation (20) with respect to x. By setting

$$f\,dx=\frac{\Gamma}{H}$$

the following expression is obtained for the field of a doublet ring:

$$\psi_0=\frac{\Gamma}{8\pi}\frac{R}{H}k\left\{x^{-1/2}\frac{k^2}{1-k^2}E(k)+x^{1/2}\left[2F(k)-\frac{2-k^2}{1-k^2}E(k)\right]\right\} \tag{21}$$

In order to obtain the effect of the entire vortex system, equation (21) is integrated with respect to h/R and x as

$$\psi\left(\frac{h}{R}\right)=\int_0^1\int_{-h/R}^{\infty}\frac{\Gamma R^2}{8\pi H}k\left\{x^{-1/2}\frac{k^2}{1-k^2}E(k)+x^{1/2}\left[2F(k)-\frac{2-k^2}{1-k^2}E(k)\right]\right\}d\frac{h}{R}\,dx \tag{22}$$

The radial velocity

$$v_R=\frac{1}{R^2}\frac{\partial\psi}{\partial\frac{h}{R}}$$

Equation (22) may be written in the form

$$\psi\left(\frac{h}{R}\right)=\frac{R^2}{8\pi H}\int_0^1\Gamma\int_{-h/R}^{\infty}\Phi\left(\frac{h}{R},\,x\right)d\frac{h}{R}\,dx \tag{23}$$

so that

$$v_R=-\frac{1}{8\pi H}\int_0^1\Gamma\,\Phi\left(-\frac{h}{R},\,x\right)dx$$

$$=-\frac{1}{8\pi H}\int_0^1\Gamma\,\Phi\left(\frac{h}{R},\,x\right)dx \tag{24}$$

Now

$$\frac{\Delta r}{R}=\frac{1}{R}\int_{\infty}^{h}\frac{dr}{dh}\,dh$$

$$=\int_{\infty}^{h/R}\frac{v_R}{V}\,d\frac{h}{R}$$

$$=\frac{1}{8\pi HV}\int_0^1\Gamma\int_{h/R}^{\infty}\Phi\left(\frac{h}{R},\,x\right)d\frac{h}{R}\,dx \tag{25}$$

By substituting

$$\Gamma=\frac{\pi c_s\lambda VR}{\kappa}K(x) \tag{26}$$

where $K(x)$ is the horizontal component of the circulation coefficient, which may be expressed as

$$K(x)=\left(\frac{x^2}{\lambda^2+x^2}\right)^{3/2} \tag{27}$$

the following equation is finally obtained:

$$\frac{\Delta r}{R}=\frac{c_s}{16\pi\kappa}\int_0^1\left(\frac{x^2}{\lambda^2+x^2}\right)^{3/2}dx\int_{h/R}^{\infty}k\left\{x^{-1/2}\frac{k^2}{1-k^2}E(k)+x^{1/2}\left[2F(k)-\frac{2-k^2}{1-k^2}E(k)\right]\right\}d\frac{h}{R} \tag{28}$$

For convenience in using the Legendre tables, the second integral is written in the form

$$\int_{h/R}^{\infty}z_1\,d\frac{h}{R} \tag{29}$$

where

$$z_1=\sin\phi\left\{\tan^2\phi\left(x^{-1/2}-x^{1/2}\right)E(k)+2x^{1/2}[F(k)-E(k)]\right\}$$

and

$$\left(\frac{h}{R}\right)^2=\frac{4x}{\sin^2\phi}-(1+x)^2$$

or

$$\phi=\sin^{-1}k$$

(See fig. 12 for plots of z_1 against h/R.)

The final expression is

$$\frac{\Delta r}{R}=\frac{c_s}{16\pi\kappa}\int_0^1\left(\frac{x^2}{\lambda^2+x^2}\right)^{3/2}dx\int_{h/R}^{\infty}\sin\phi\left\{\tan^2\phi\left(x^{-1/2}-x^{1/2}\right)E(k)+2x^{1/2}[F(k)-E(k)]\right\}d\frac{h}{R}$$

(See table VII and fig. 13.)

INFINITE NUMBER OF BLADES FOR DUAL ROTATION

The contraction for a dual-rotating propeller with an infinite number of blades is next obtained. In this case $K(x)=1$, and the radial velocity is

$$v_R=-\frac{\Gamma}{2\pi H}\left[x^{1/2}\left\{\left(\frac{2}{k}-k\right)F(k)-\frac{2}{k}E(k)\right\}\right]_{x=0}^{x=1}$$

Since the value at the lower limit is zero and $K(x)=1$ for an infinite number of blades, it follows by substituting the value of Γ that

$$\frac{\Delta r}{R}=-\frac{c_s}{4\pi}\int_{h/R}^{\infty}w_1\,d\frac{h}{R}$$

where

$$w_1=\left[\left(\frac{2}{k}-k\right)F(k)-\frac{2}{k}E(k)\right]^{x=1}$$

(See table VIII and fig. 14.)

CONCLUDING REMARKS

The contraction coefficients are given for two-blade and four-blade single-rotating propellers at four specific values of the advance ratio. The calculations involve triple integrations and are therefore somewhat laborious and susceptible to numerical errors. Until more convenient methods are devised to perform this integration, it is hoped that the values given in this paper will serve the purpose. It is well to notice the small magnitude of the contraction. A four-blade propeller with normal loading and advance ratio is shown to have a total contraction in terms of the radius of less than one percent. The first-order treatment embodied in the paper is therefore adequate for all technical purposes.

LANGLEY MEMORIAL AERONAUTICAL LABORATORY,
NATIONAL ADVISORY COMMITTEE FOR AERONAUTICS,
LANGLEY FIELD, VA., *October 10, 1944.*

REFERENCE

1. Lamb, Horace: Hydrodynamics. Sixth ed., Cambridge Univ. Press, 1932.

TABLE I.—FUNCTION $\frac{\lambda^3}{4}Y_1$ FOR TWO-BLADE PROPELLER

θ (deg)	$\frac{\lambda^3}{4}Y_1$	θ (deg)	$\frac{\lambda^3}{4}Y_1$		
	$\lambda=\frac{1}{4}$		$\lambda=\frac{1}{2}$	$\lambda=1$	$\lambda=1\frac{1}{2}$
50	−0.000291	1	−0.000138	----------	−0.000683
100	.000148	2	−.000213	−0.000282	−.001088
130	.001966	3	−.000293	----------	−.001367
150	.004813	4	−.000382	----------	−.001232
170	.006679	5	−.000488	----------	−.001283
200	.005052	6	−.000570	−.000923	−.001316
220	.002008	7	−.000682	----------	−.001358
250	.000730	8	−.000789	----------	−.001358
300	.000450	9	−.000898	----------	−.001350
350	.001305	10	−.000984	−.001792	−.001358
400	.000622	20	−.001139	−.001571	−.001367
500	.000270	40	−.000999	−.001286	−.001080
550	.000400	60	−.000802	−.000862	−.000759
600	.000145	80	−.000339	−.000324	−.000354
650	.000031	100	.000460	.000312	.000084
700	.000149	120	.001730	.000709	.000274
750	.000175	140	.003131	.000809	.000347
800	.000058	160	.003351	.000740	.000321
900	.000079	180	.002658	.000492	.000132
		200	.001544	.000237	.000100
		220	.000625	.000093	.000073
		240	.000160	.000014	−.000015
		260	−.000056	.000003	.000008
		280	.000049	−.000013	.000036
		300	.000213	−.000004	.000047
		320	.000363	.000004	.000036
		340	.000390	.000008	.000030
		360	.000343	.000031	.000001
		380	.000232	.000008	−.000003
		400	.000113	−.000003	.000004
		420	.000027	.000020	.000007
		440	−.000011	6.000011	
		460	.000014		

TABLE II.—FUNCTION $\frac{\lambda^3}{4}Y_1$ FOR FOUR-BLADE PROPELLER

θ (deg)	$\frac{\lambda^3}{4}Y_1$	θ (deg)	$\frac{\lambda^3}{4}Y_1$		
	$\lambda=\frac{1}{4}$		$\lambda=\frac{1}{2}$	$\lambda=1$	$\lambda=1\frac{1}{2}$
0	0.000500	1	----------	----------	−0.000273
10	−.020680	2	----------	−0.000001	−.000250
30	.097700	3	----------	----------	−.000088
60	1.251120	4	----------	----------	.000083
65	1.858120	5	−0.004211	----------	.000251
70	2.879450	6	----------	.000002	.000501
75	3.849270	7	----------	----------	.000704
80	4.594600	8	----------	----------	.000905
85	4.987600	9	----------	----------	.001263
90	4.538300	10	−.011374	−.000013	.001432
95	3.549380	20	.006150	.001786	.002984
100	2.685010	40	.137004	.006466	.005328
110	1.330560	60	.363018	.006423	.003108
120	.821510	80	.342699	.004174	.001577
160	1.017150	100	.218548	.002161	.000532
200	.902770	120	.112735	.001281	.000298
250	.436960	140	.091686	.000865	.000224
300	.323530	160	.075117	.000535	.000214
350	.217700	180	.058218	.000345	.000166
400	.154190	200	.040861	.000224	.000078
450	.154010	220	.030023	.000176	.000101
500	.119570	240	.024839	.000130	.000066
550	.038450	260	.021139	.000100	.000057
600	−.029500	280	.017093	.000062	.000048
		300	.014048	.000042	.000037
		320	.011174	.000032	.000025
		340	.009069	.000016	.000002
		360	.007762	.000032	.000004
		380	.006439	−.000018	
		400	.004650	−.000041	
		420	.003748	−.000003	
		440	.003884	−.000004	
		460	.004428		

TABLE III.—FUNCTION $\frac{\lambda^3}{4}Y_2$ FOR TWO-BLADE PROPELLER

θ (deg)	$\frac{\lambda^3}{4}Y_2$	θ (deg)	$\frac{\lambda^3}{4}Y_2$		
	$\lambda=\frac{1}{4}$		$\lambda=\frac{1}{2}$	$\lambda=1$	$\lambda=1\frac{1}{2}$
0	8.138900	0	0.377250	−0.004494	−0.003136
20	8.159900	2	.377650	−.004435	----------
40	8.219400	4	.378580	−.004280	----------
60	8.291400	6	.380140	−.003990	----------
80	8.351400	8	.382320	−.003490	----------
100	8.358900	10	.385170	−.002790	−.002466
120	8.223900	20	.402420	.000595	−.001651
140	7.745900	30	----------	----------	−.000876
160	6.570900	40	.437620	.006355	−.000189
180	4.917900	50	----------	----------	.000407
200	3.412900	60	.467020	.010675	.000907
220	2.512900	70	----------	----------	.001302
240	2.232900	80	.486770	.013075	.001577
260	2.202900	90	----------	----------	.001717
280	2.245900	100	.485670	.013075	.001724
300	2.215900	120	.453070	.011070	.001504
320	2.026900	140	.373150	.008050	.001129
340	1.734900	160	.267250	.004870	.000718
360	1.404900	180	.169400	.002470	.000444
380	1.108400	200	.102200	.001070	.000313
400	.890900	220	.067320	.000470	.000207
420	.780400	240	.055310	.000280	.000178
440	.745400	260	.053460	.000270	.000189
460	.740400	280	.052810	.000280	.000162
500	.674400	300	.048820	.000290	.000112
540	.504400	320	.040500	.000290	.000065
580	.324400	340	.028630	.000260	.000025
620	.246400	360	.016630	.000150	.000007
660	.231400	380	.007610	.000090	.000007
700	.189400	400	.002400	.000080	.000006
740	.112000	420	.000420	.000070	
780	.030000	440	.000100		
820	−.006000				
860	−.004000				

TABLE IV.—FUNCTION $\frac{\lambda^3}{4}Y_2$ FOR FOUR-BLADE PROPELLER

θ (deg)	$\frac{\lambda^3}{4}Y_2$	θ (deg)	$\frac{\lambda^3}{4}Y_2$		
	$\lambda=\frac{1}{4}$		$\lambda=\frac{1}{2}$	$\lambda=1$	$\lambda=1\frac{1}{2}$
0	0.024414	0	0.017258	0.007918	0.005175
10	.024414	2	.017259	.007918	.005107
20	.024416	4	.017261	.007918	.004728
30	.024380	6	.017266	.007918	.004084
40	.024256	8	.017276	.007918	.003214
50	.023969	10	.017287	.007918	.002343
60	.023338	20	.017317	.007908	.001099
70	.021958	40	.016676	.006873	.001235
80	.019333	60	.013899	.004520	.000902
90	.016049	80	.009902	.002668	.000675
100	.013540	100	.006845	.001594	.000541
110	.012166	120	.005099	.001014	.000404
130	.010889	140	.004010	.000644	.000314
150	.009821	160	.003112	.000407	.000240
170	.008444	180	.002383	.000255	.000173
190	.006951	200	.001859	.000157	.000135
210	.005703	220	.001486	.000091	.000102
230	.004773	240	.001186	.000037	.000073
250	.004082	260	.000949	.000049	.000052
270	.003528	280	.000744	.000028	.000035
290	.003035	300	.000596	.000010	.000020
310	.002594	320	.000472	−.000002	.000009
330	.002216	340	.000363	−.000010	.000003
350	.001887	360	.000271	−.000019	
370	.001612	380	.000192	−.000021	
390	.001376	400	.000132	−.000013	
410	.001166	420	.000087	−.000001	
430	.000959	440	.000046		
450	.000754				
470	.000550				
490	.000367				
510	.000205				
530	.000075				

TABLE V.—FUNCTION $\frac{\lambda^3}{4}Y_3$ FOR TWO-BLADE PROPELLER

θ (deg)	$\frac{\lambda^3}{4}Y_3$	θ (deg)	$\frac{\lambda^3}{4}Y_3$		
	$\lambda=\frac{1}{4}$		$\lambda=\frac{1}{2}$	$\lambda=1$	$\lambda=1\frac{1}{2}$
0	0.048613	0	0.015944	0.002141	0.000602
20	.044739	2	.015800	.002154	----------
40	.040850	4	.015656	.002168	----------
60	.036926	6	.015511	.002180	----------
80	.032975	8	.015366	.002191	----------
100	.029007	10	.015221	.002201	.000748
120	.025056	20	.014474	.002217	.000855
140	.021248	30	-------	-------	.000921
160	.017800	40	.012913	.002111	.000950
180	.015057	50	-------	-------	.000944
200	.013062	60	.011197	.001852	.000910
220	.011670	70	-------	-------	.000854
240	.010549	80	.009382	.001490	.000780
260	.009501	90	-------	-------	.000695
280	.008448	100	.007525	.001094	.000607
300	.007392	120	.005732	.000728	.000439
320	.006381	140	.004148	.000437	.000303
340	.005483	160	.002927	.000243	.000208
360	.004734	180	.002099	.000136	.000148
380	.004139	200	.001594	.000087	.000111
400	.003664	220	.001277	.000065	.000086
420	.003268	240	.001049	.000055	.000066
440	.002903	260	.000837	.000047	.000048
460	.002459	280	.000632	.000039	.000030
500	.001882	300	.000441	.000031	.000017
540	.001318	320	.000276	.000022	.000007
580	.000922	340	.000146	.000014	.000002
620	.000651	360	.000066	.000008	.000001
660	.000425	380	.000021	.000005	.000001
700	.000232	400	.000005	.000002	
740	.000085	420	.000001		
780	−.000006				
820	−.000005				

TABLE VI.—FUNCTION $\frac{\lambda^3}{4}Y_3$ FOR FOUR-BLADE PROPELLER

θ (deg)	$\frac{\lambda^3}{4}Y_3$	θ (deg)	$\frac{\lambda^3}{4}Y_3$		
	$\lambda=\frac{1}{4}$		$\lambda=\frac{1}{2}$	$\lambda=1$	$\lambda=1\frac{1}{2}$
0	0.067786	0	0.033572	0.010513	0.005286
10	.063525	2	.032969	.010236	----------
20	.059264	4	.032367	.009960	----------
30	.055006	6	.031764	.009684	----------
40	.050757	8	.031162	.009407	----------
50	.046549	10	.030558	.009131	.004389
60	.042420	20	.027537	.007750	.003532
70	.038450	30	----------	----------	.002766
80	.034832	40	.021584	.005158	.002131
90	.031732	50	----------	----------	.001650
100	.029167	60	.016211	.003155	.001297
110	.026892	70	----------	----------	.001040
130	.022885	80	.012055	.001916	.000856
150	.019263	90	----------	----------	.000722
170	.016059	100	.009157	.001185	.000618
190	.013358	120	.007100	.000738	.000465
210	.011148	140	.005512	.000453	.000343
230	.009303	160	.004265	.000267	.000243
250	.007765	180	.003314	.000151	.000173
270	.006435	200	.002574	.000086	.000122
290	.005288	220	.002003	.000052	.000080
310	.004300	240	.001545	.000022	.000049
330	.003461	260	.001165	−.000000	.000029
350	.002748	280	.000863	−.000012	.000015
370	.002138	300	.000634	−.000019	.000006
390	.001621	320	.000452	−.000021	.000002
410	.001181	340	.000307	−.000019	
430	.000823	360	.000196	−.000014	
450	.000532	380	.000116	−.000008	
470	.000306	400	.000061	−.000002	
490	.000153	420	.000023		
510	.000052				

TABLE VII.—CONTOUR LINES—SINGLE-ROTATING PROPELLER

h/R	$\frac{\Delta r}{R}\frac{1}{c_s}$	h/R	$\frac{\Delta r}{R}\frac{1}{c_s}$	h/R	$\frac{\Delta r}{R}\frac{1}{c_s}$	h/R	$\frac{\Delta r}{R}\frac{1}{c_s}$
	$\lambda=\frac{1}{4}$		$\lambda=\frac{1}{2}$		$\lambda=1$		$\lambda=1\frac{1}{2}$
4.0	0.00045	4.0	0.00060	4.0	0.00058	4.0	0.00032
3.0	.00263	3.0	.00226	3.0	.00188	3.0	.00148
2.0	.00747	2.6	.00350	2.6	.00292	2.6	.00226
1.6	.01148	2.2	.00545	2.2	.00424	2.2	.00332
1.2	.01796	1.8	.00838	1.8	.00626	1.8	.00487
.8	.02888	1.4	.01266	1.4	.00937	1.4	.00726
.45	.04733	1.0	.01963	1.0	.01446	1.0	.01107
		.8	.02499	.8	.01812	.6	.01768
		.6	.03247	.6	.02312	.45	.02330
		.4	.04312	.4	.03053		
		.2	.05997	.2	.04233		
		.1	.07388	.12	.04985		

TABLE VIII.—CONTOUR LINES—DUAL-ROTATING PROPELLER

h/R	$\frac{\Delta r}{R}\frac{1}{c_s}$
10.00	0.000060
9.50	.000141
9.00	.000244
8.50	.000368
8.00	.000513
7.50	.000680
7.00	.000867
6.50	.001074
6.00	.001472
5.50	.001898
5.00	.002355
4.50	.002873
4.00	.003716
3.50	.004671
3.00	.006183
2.50	.008889
2.00	.013390
1.75	.016370
1.50	.020350
1.25	.025820
1.00	.033490
.75	.044930
.50	.062340
.45	.066120
.40	.070340
.35	.075070
.30	.080400
.25	.086370
.20	.093230
.15	.101230
.10	.110680
.05	.123220

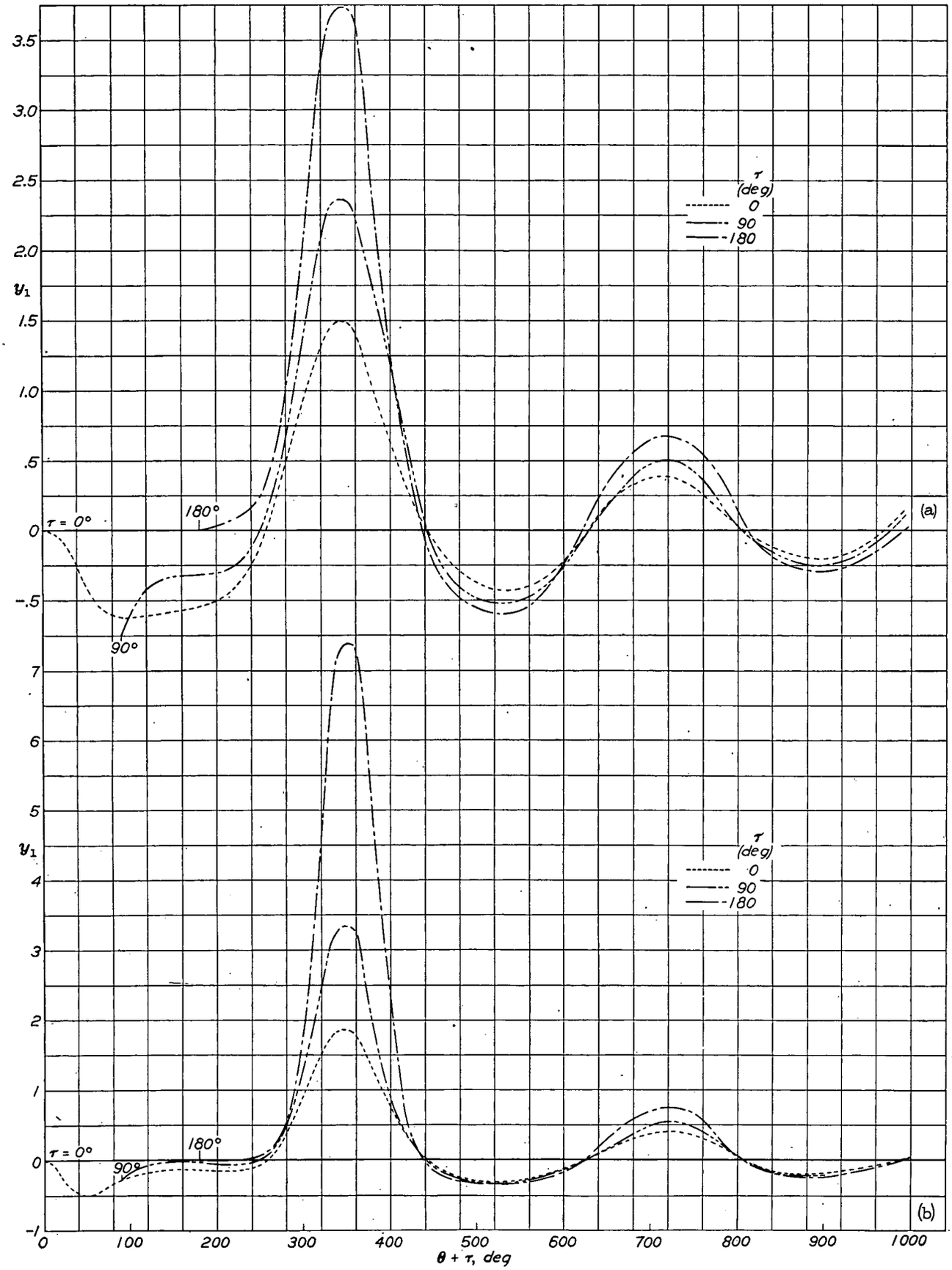

(a) $x=¼$. (b) $x=½$.

FIGURE 3.—The function y_1 for $\lambda=¼$ and four values of τ.

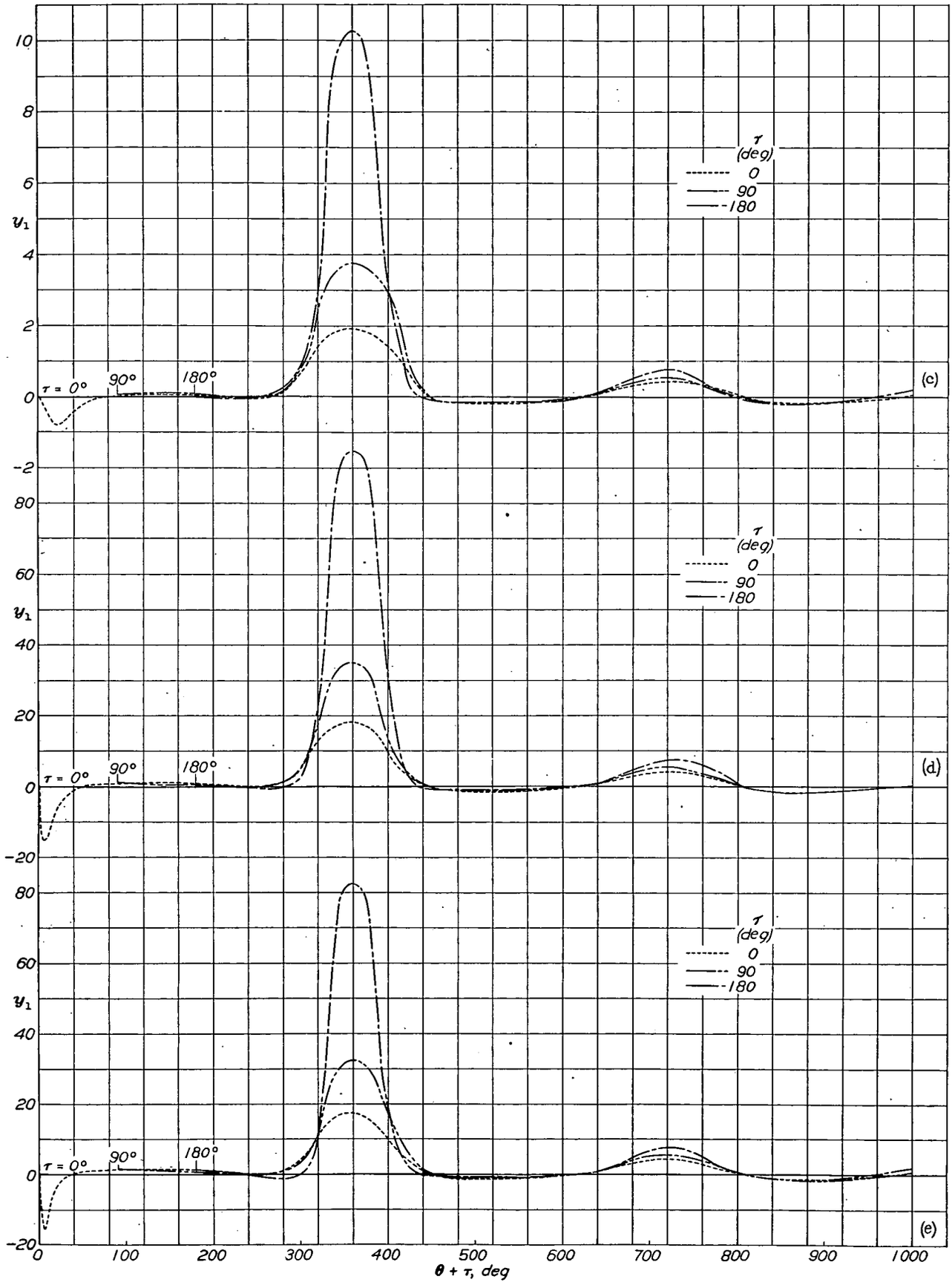

(c) $x=\frac{3}{4}$. (d) $x=\frac{7}{8}$. (e) $x=\frac{15}{16}$.

FIGURE 3.—Continued.

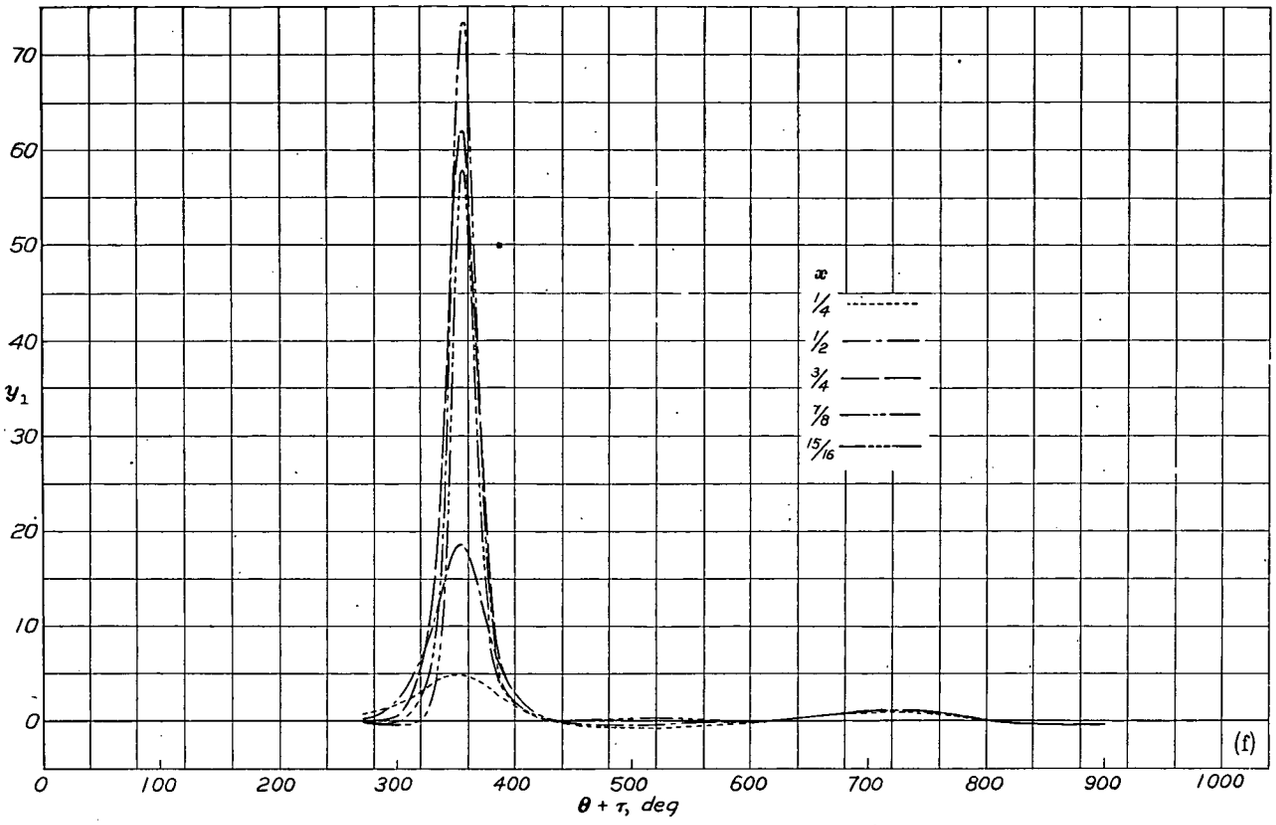

(f) $x=¼$, ½, ¾, ⅞, and 15⁄16; $\tau=270°$.

FIGURE 3.—Concluded.

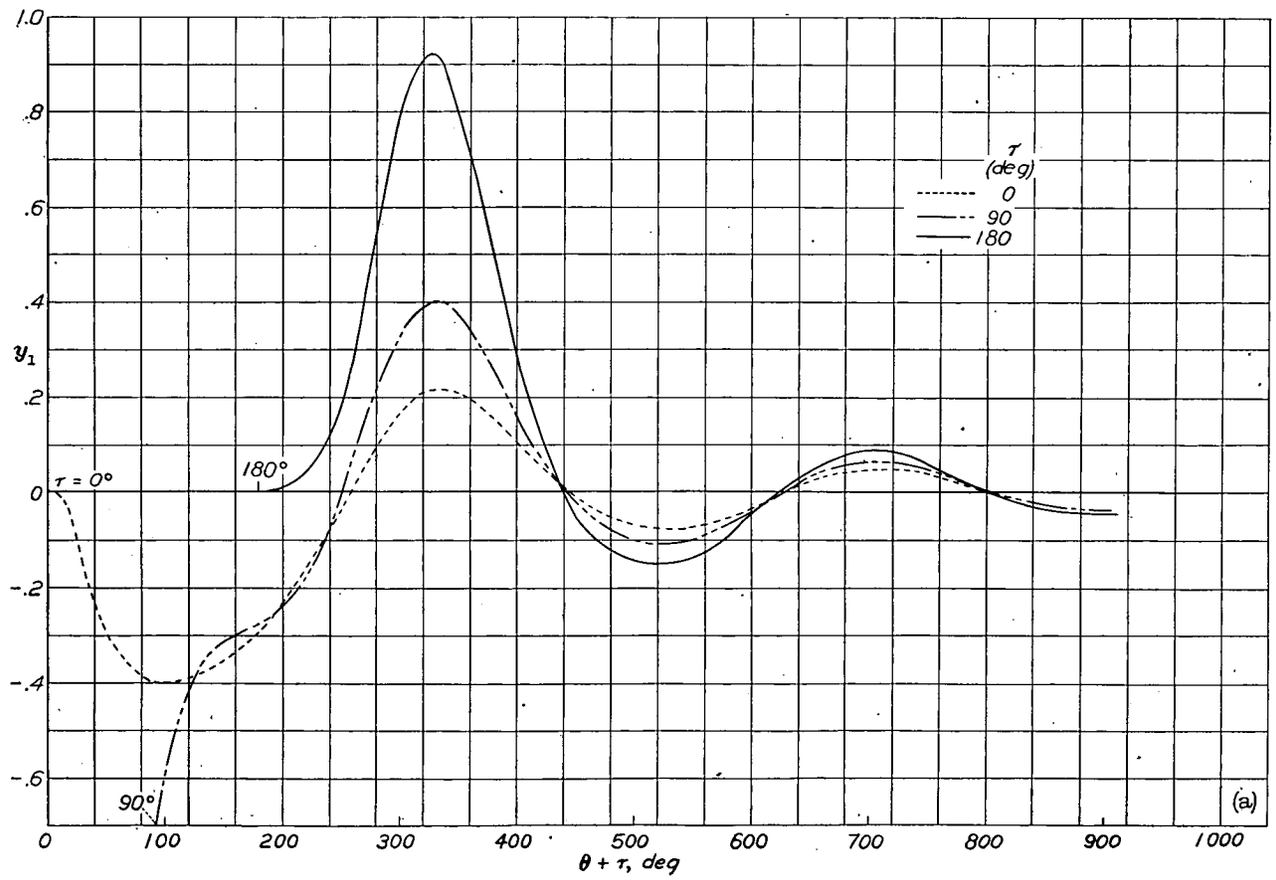

(a) $x=¼$.

FIGURE 4.—The function y_1 for $\lambda=½$ and four values of τ.

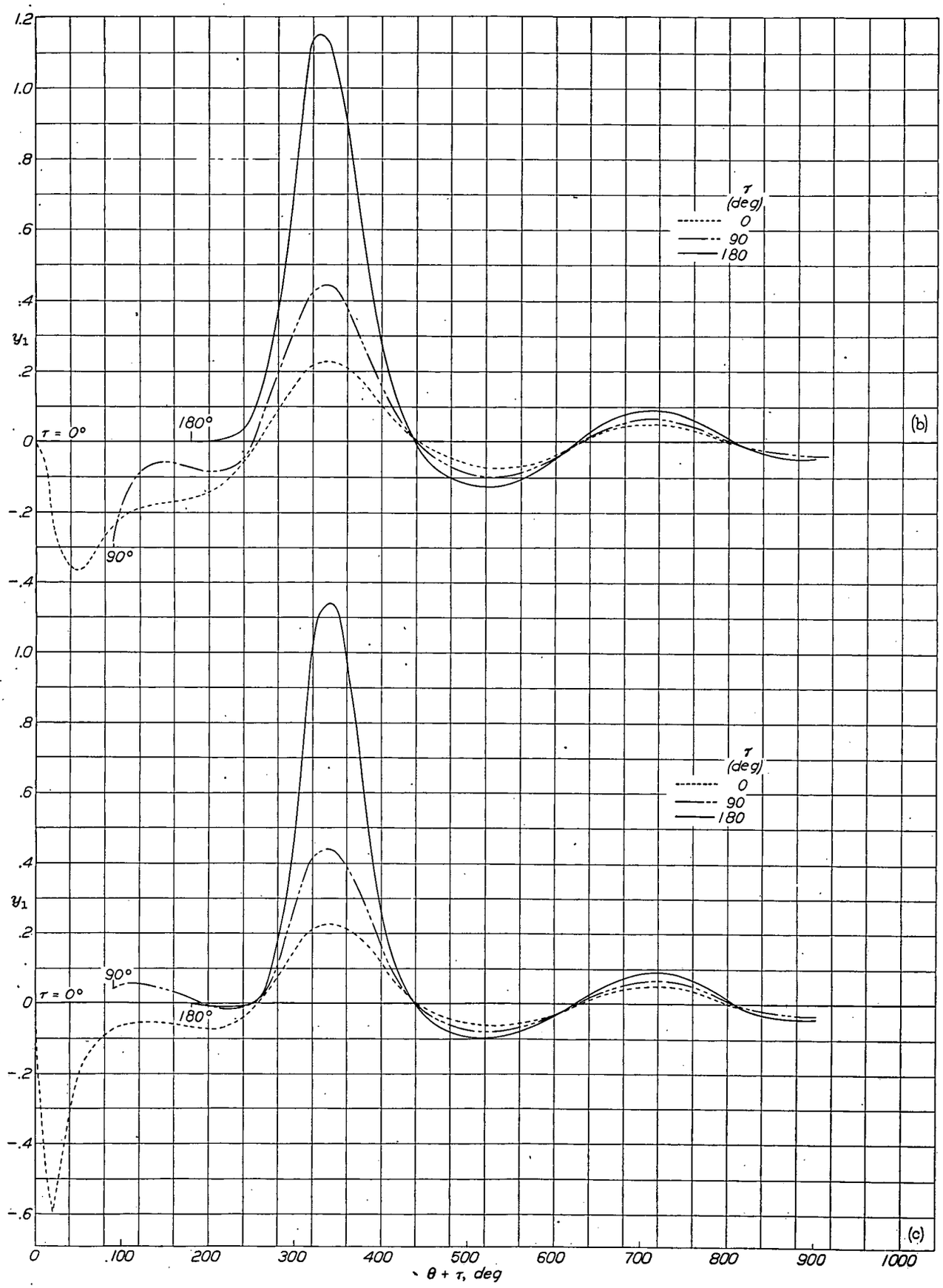

(b) $x=\frac{1}{2}$.

(c) $x=\frac{3}{4}$.

FIGURE 4.—Continued.

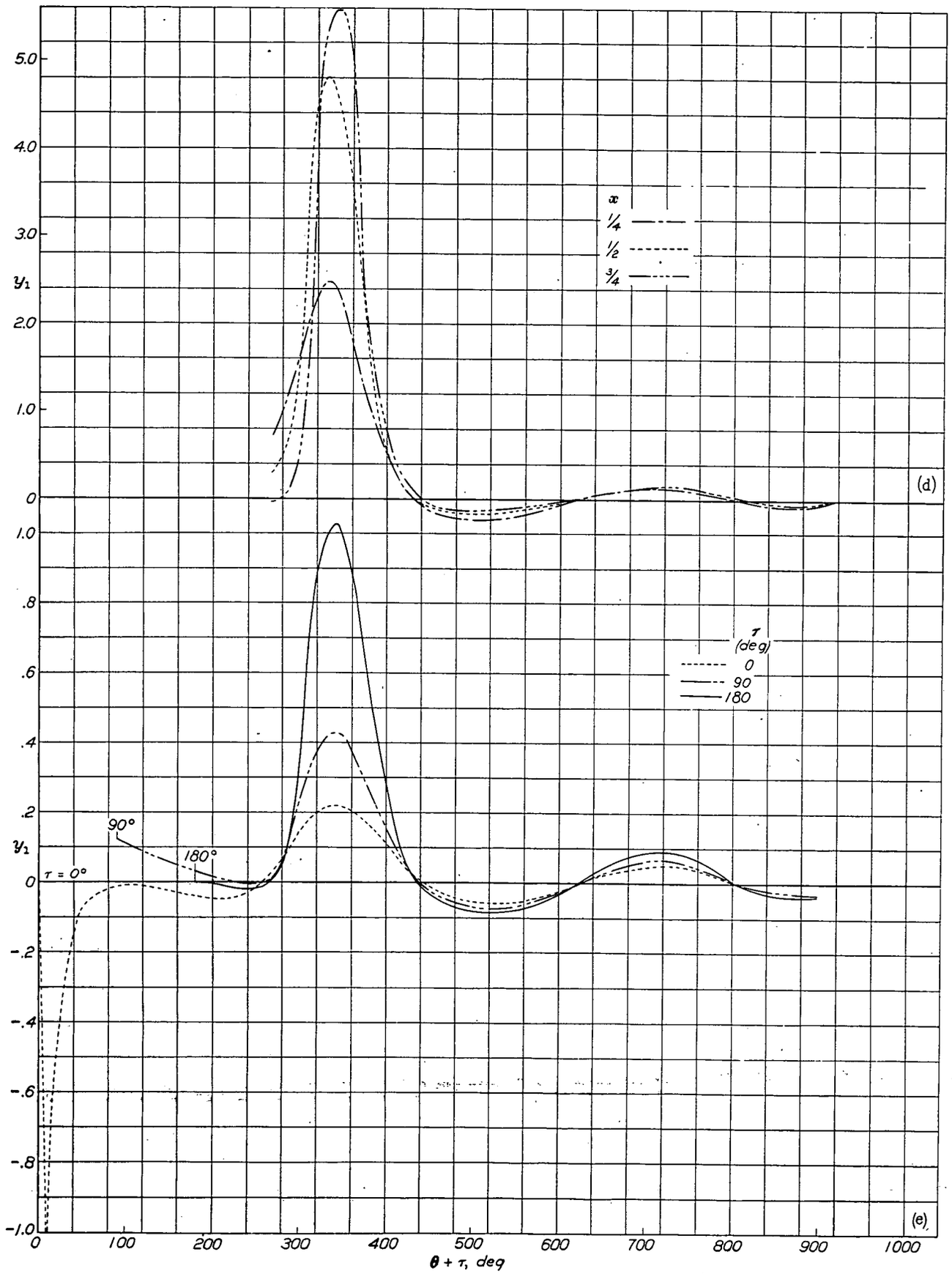

(d) $x = \frac{1}{4}, \frac{1}{2}$, and $\frac{3}{4}$; $\tau = 270°$.

(e) $x = \frac{7}{8}$.

FIGURE 4.—Continued.

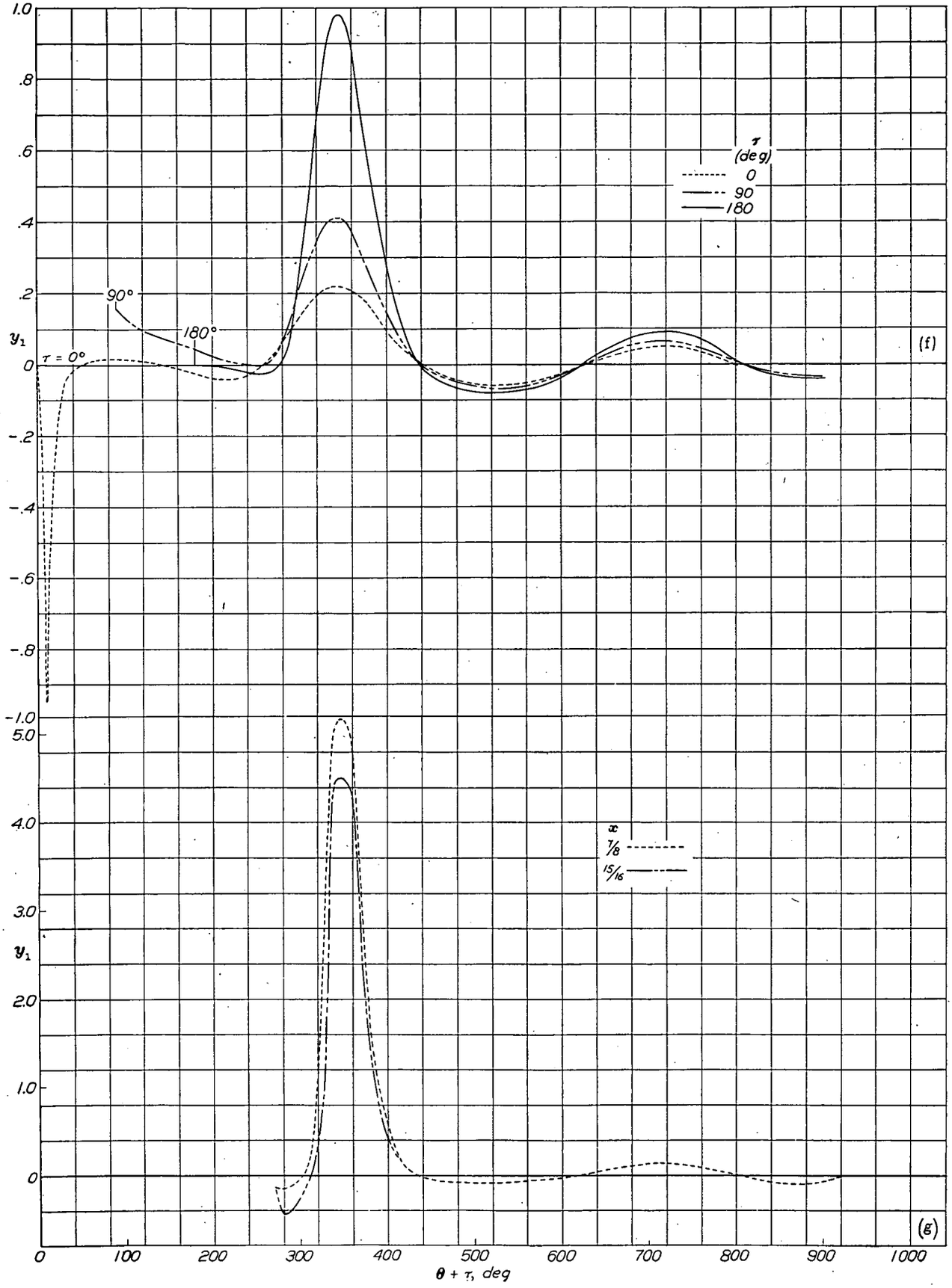

(f) $x = 15/16$.

(g) $x = 7/8$ and $15/16$; $\tau = 270°$.

FIGURE 4.—Concluded.

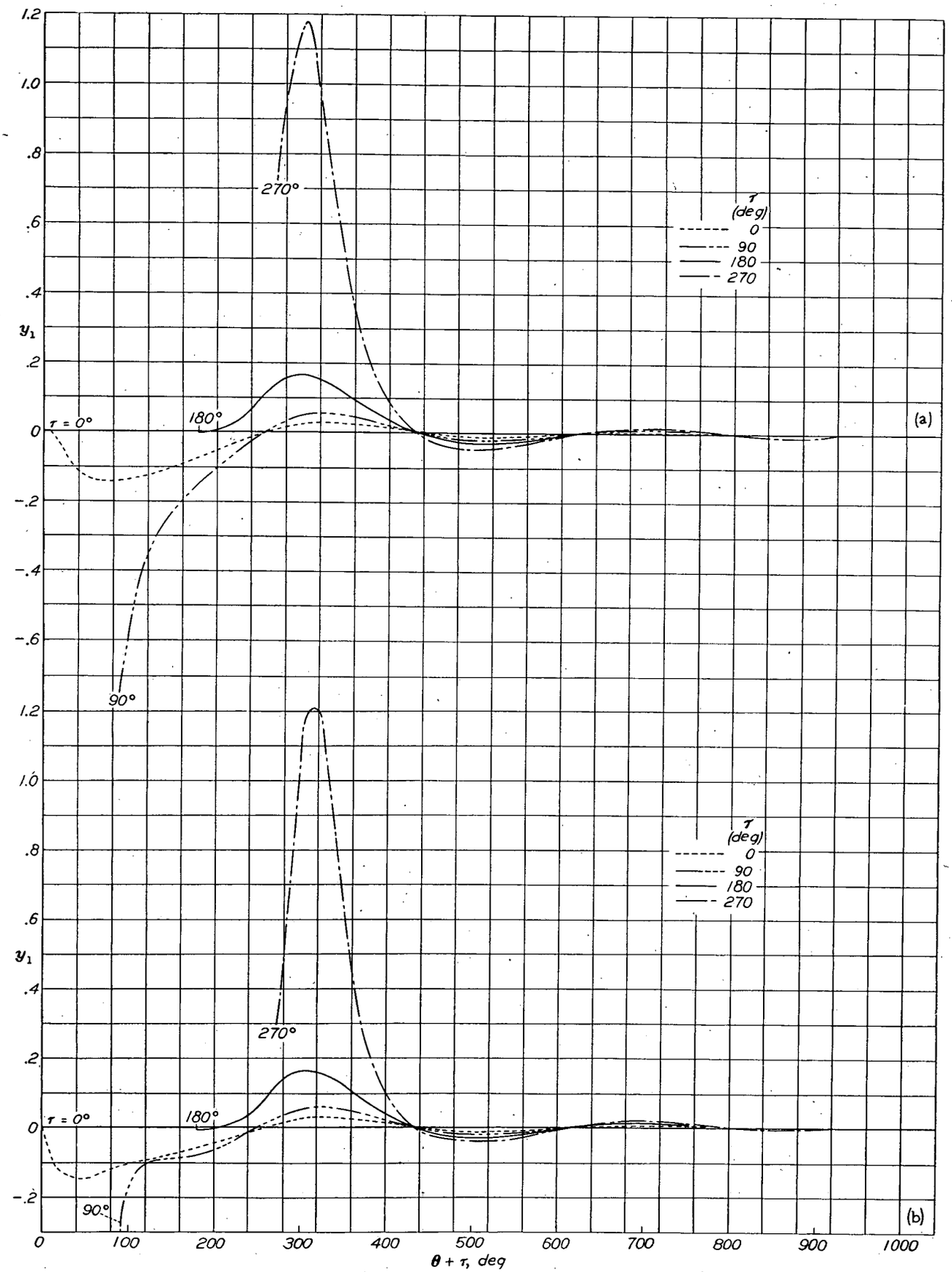

(a) $x = \frac{1}{4}$. (b) $x = \frac{1}{2}$.

FIGURE 5.—The function y_1 for $\lambda = 1$ and four values of τ.

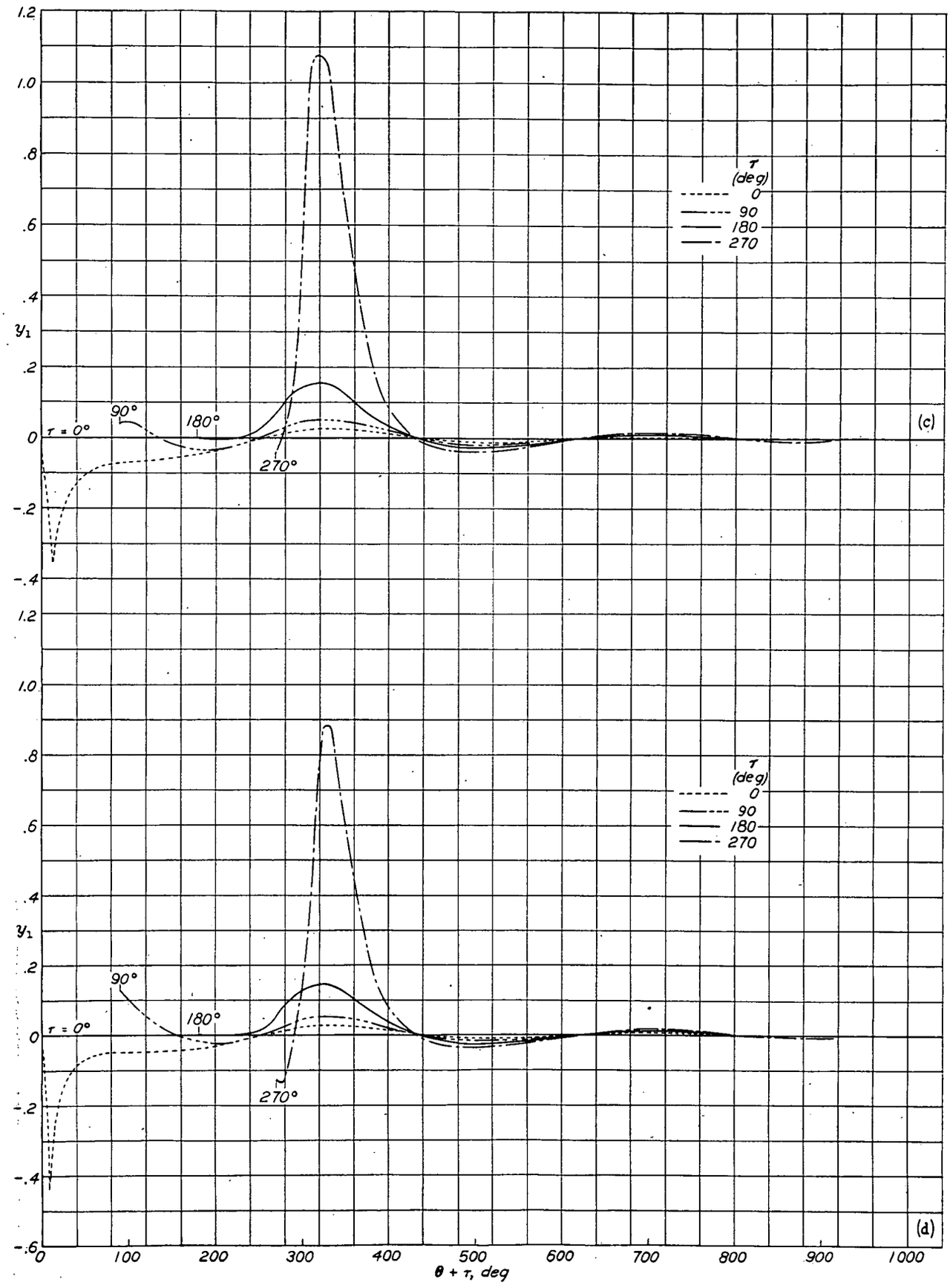

(c) $\tau = \frac{3}{4}$.

(d) $\tau = \frac{7}{8}$.

FIGURE 5.—Continued.

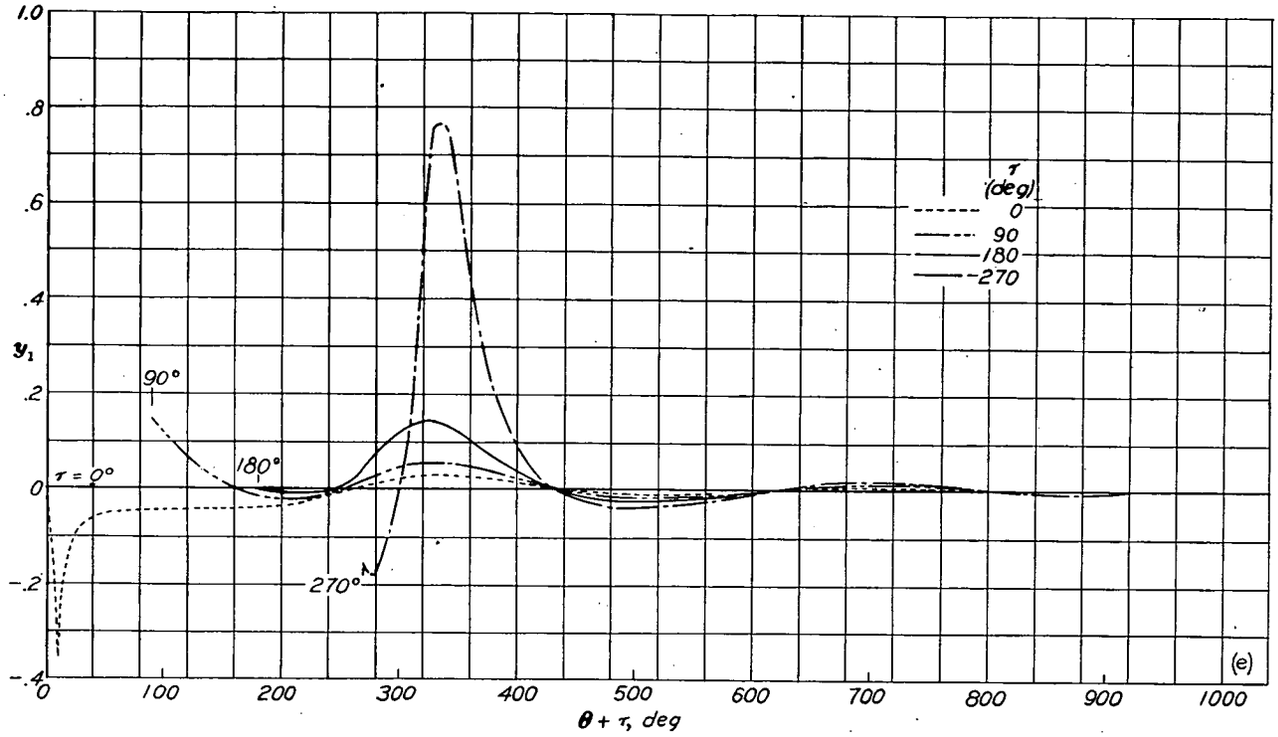

(e) $x = 15/16$.

FIGURE 5.—Concluded.

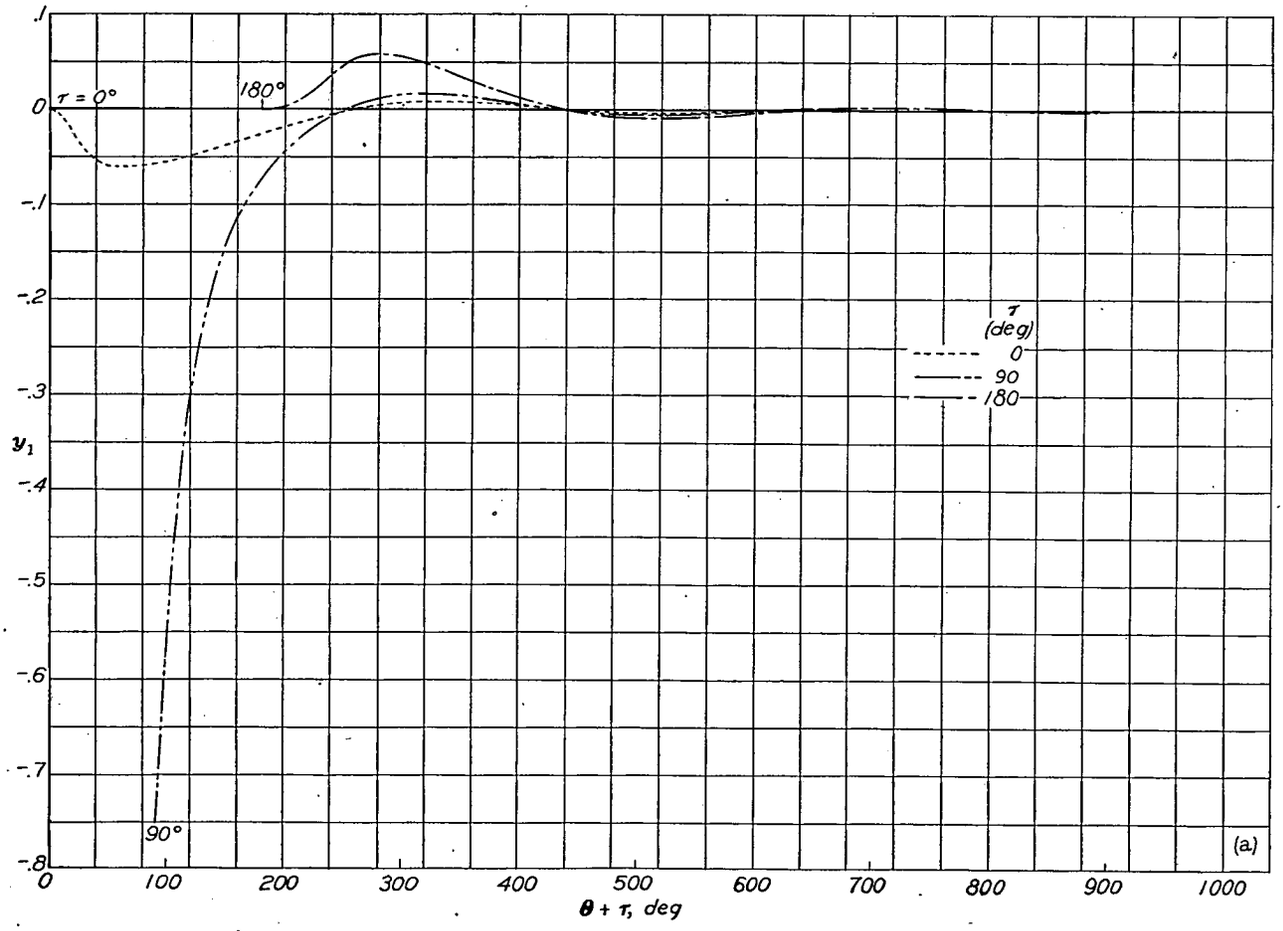

(a) $x = 1/4$.

FIGURE 6.—The function y_1 for $\lambda = 1\frac{1}{2}$ and four values of τ.

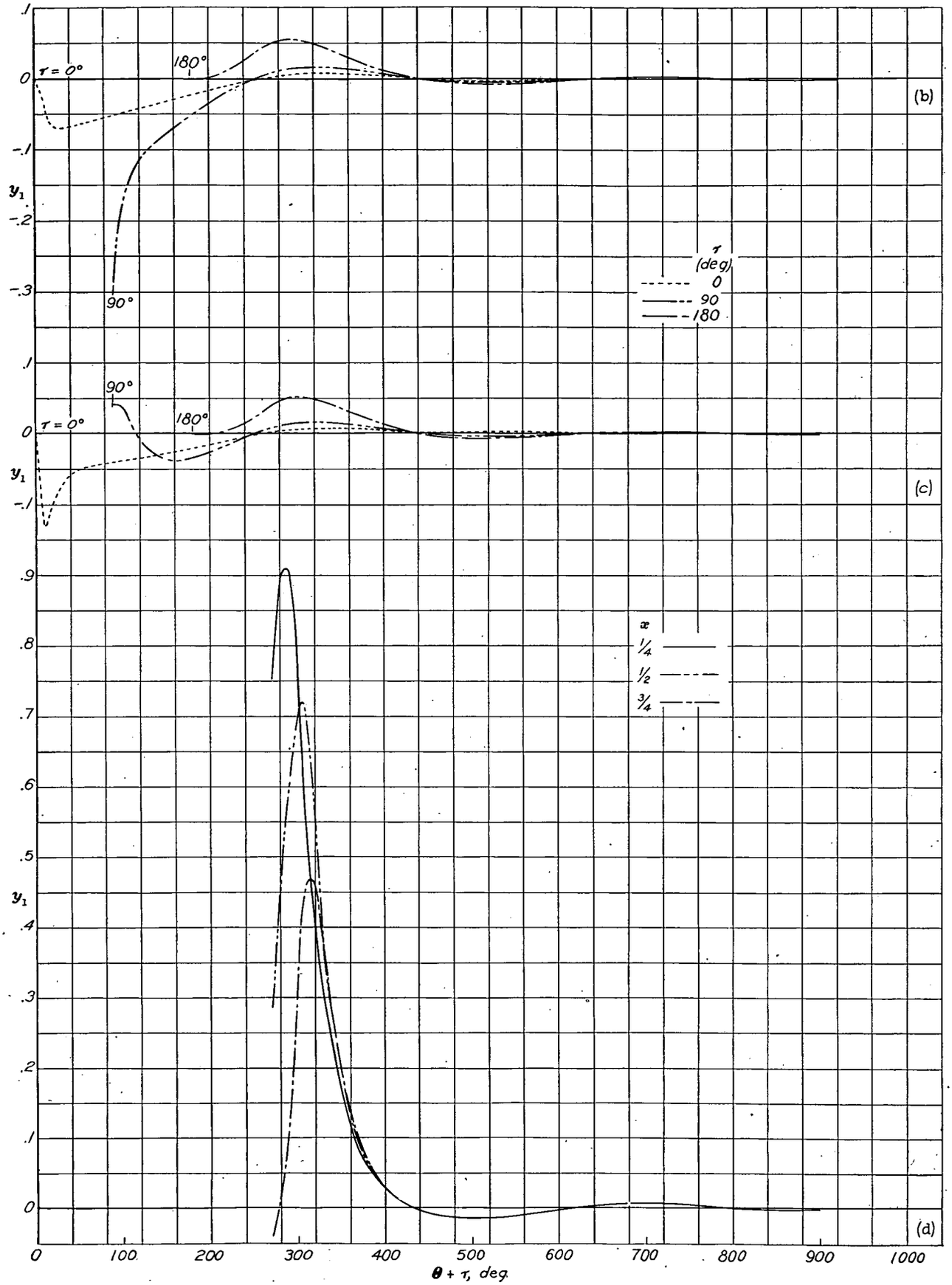

(b) $x=½$. (c) $x=¾$. (d) $x=¼$, ½, and ¾; $\tau=270°$.

FIGURE 6.—Continued.

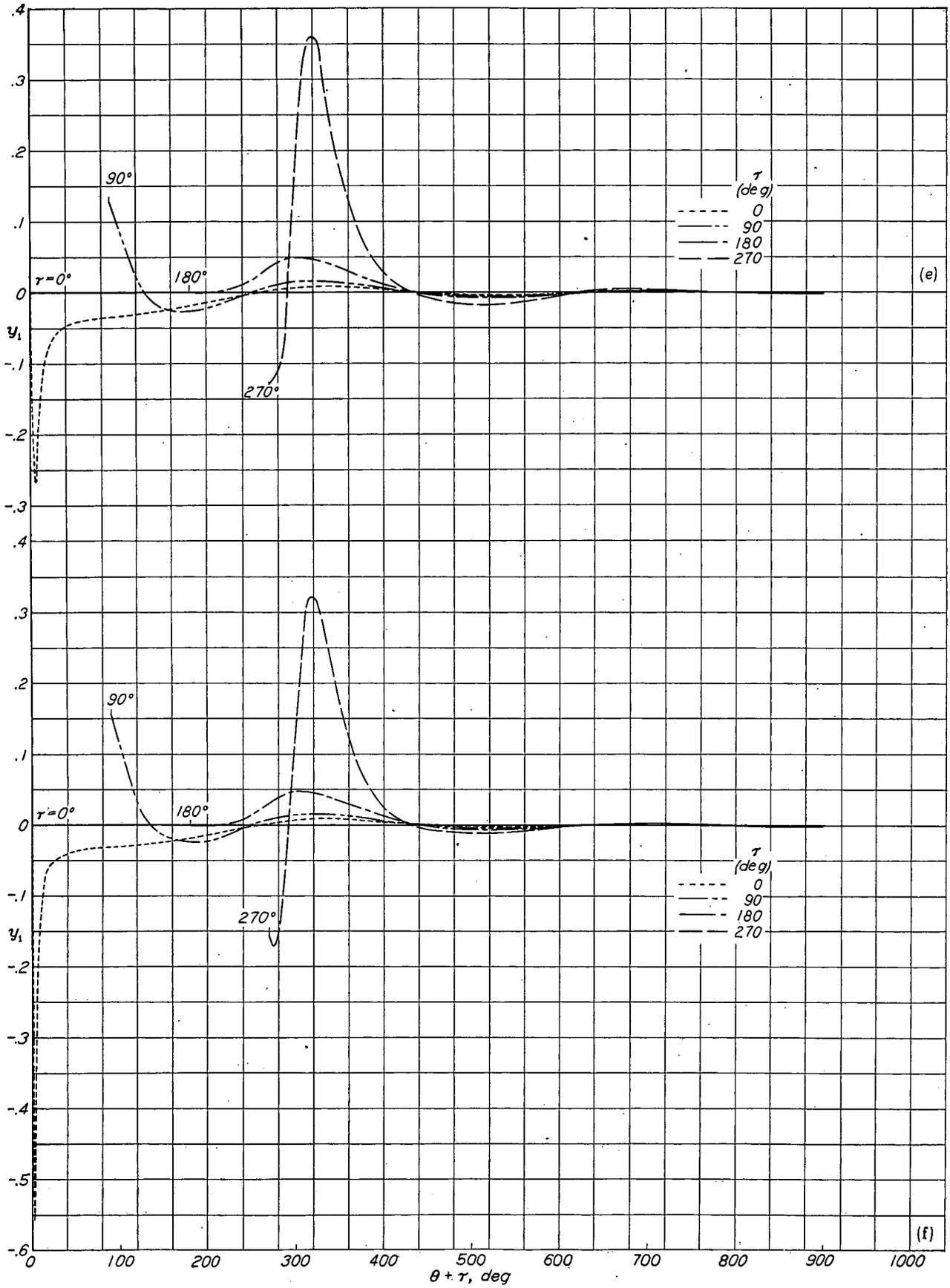

(e) $x=\frac{7}{8}$.

(f) $x=1\frac{15}{16}$.

FIGURE 6.—Concluded.

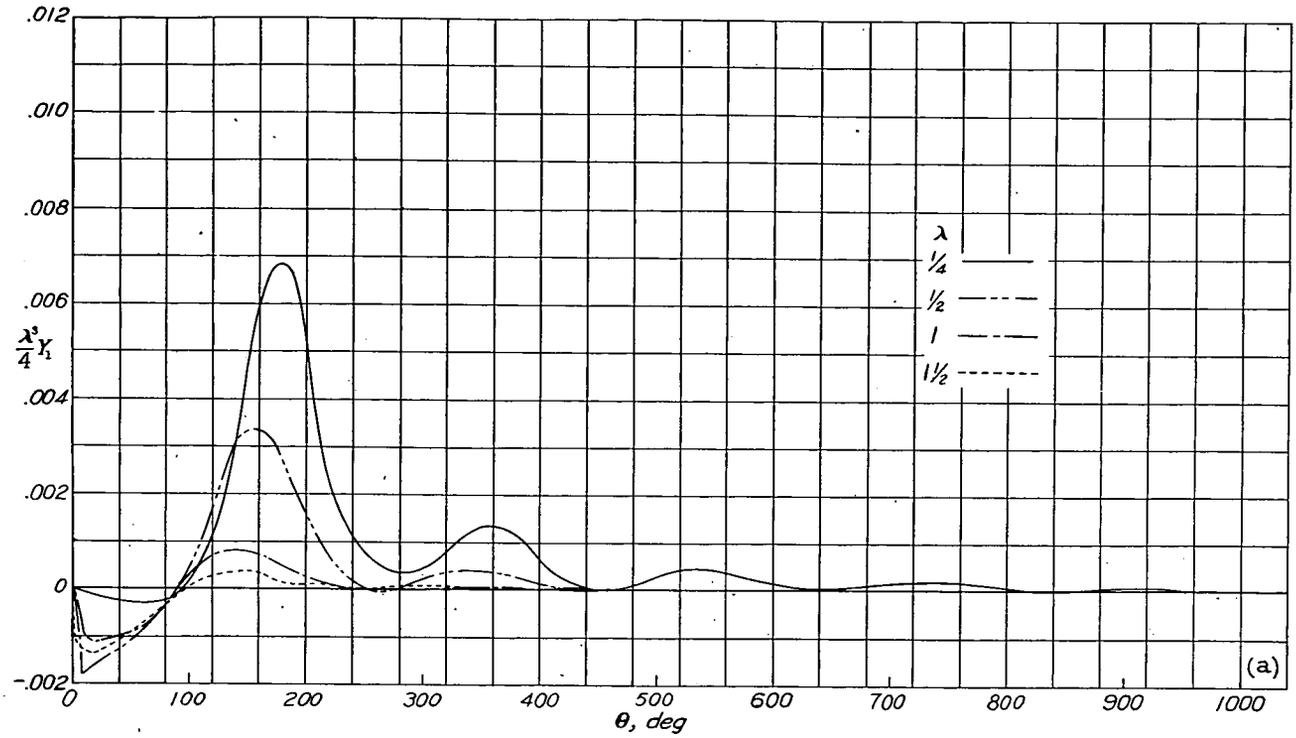

(a) Two-blade propeller. (See table I.)

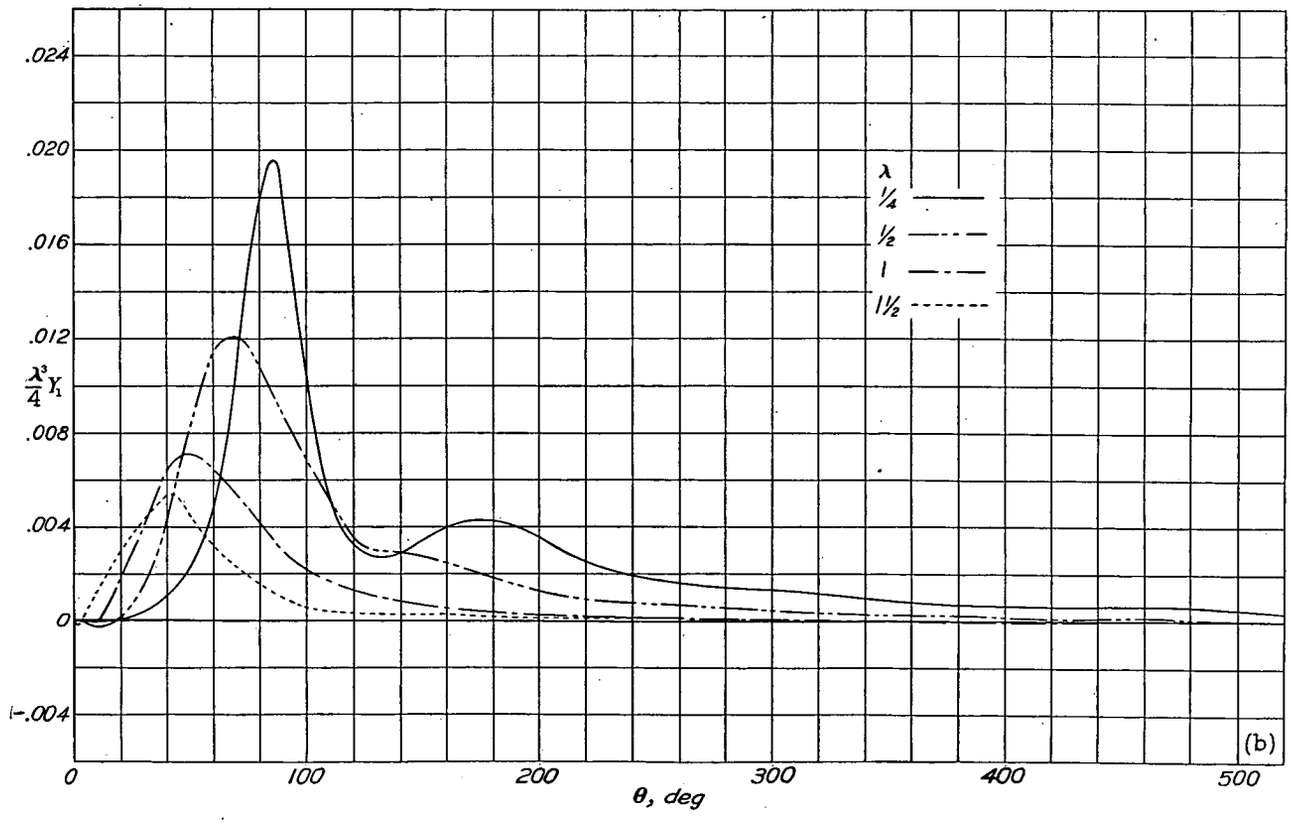

(b) Four-blade propeller. (See table II.)

FIGURE 7.—The function $\frac{\lambda^3}{4}Y_1$ against θ for four values of λ.

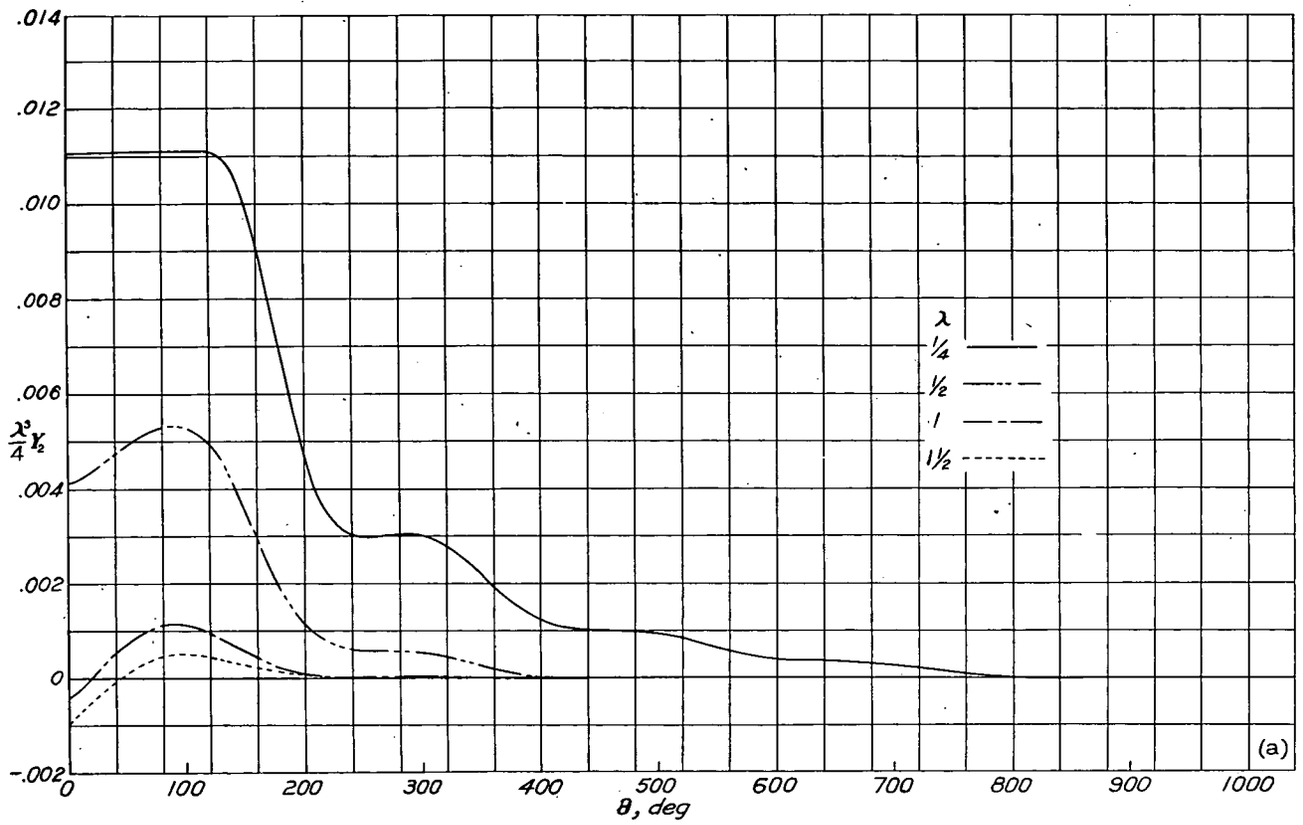

(a) Two-blade propeller. (See table III.)

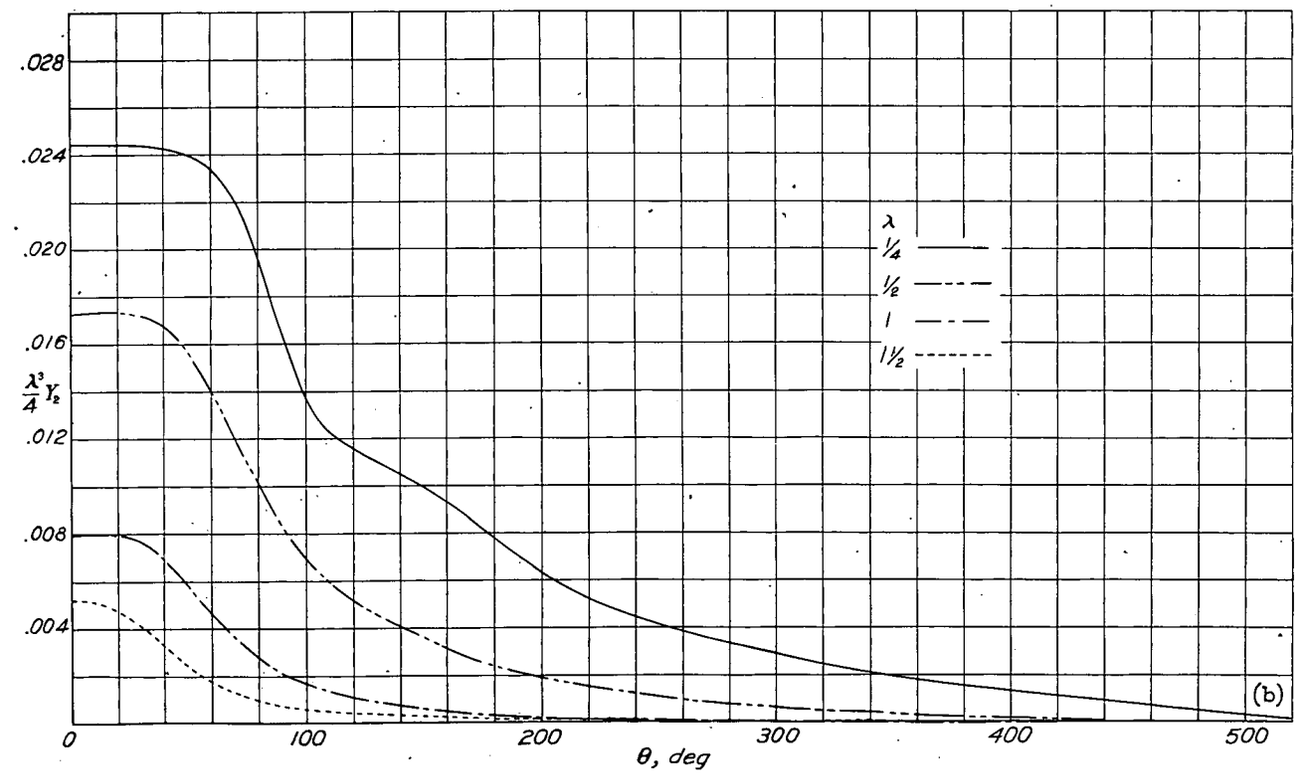

(b) Four-blade propeller. (See table IV.)

FIGURE 8.—The function $\frac{\lambda^3}{4}Y_2$ against θ for four values of λ.

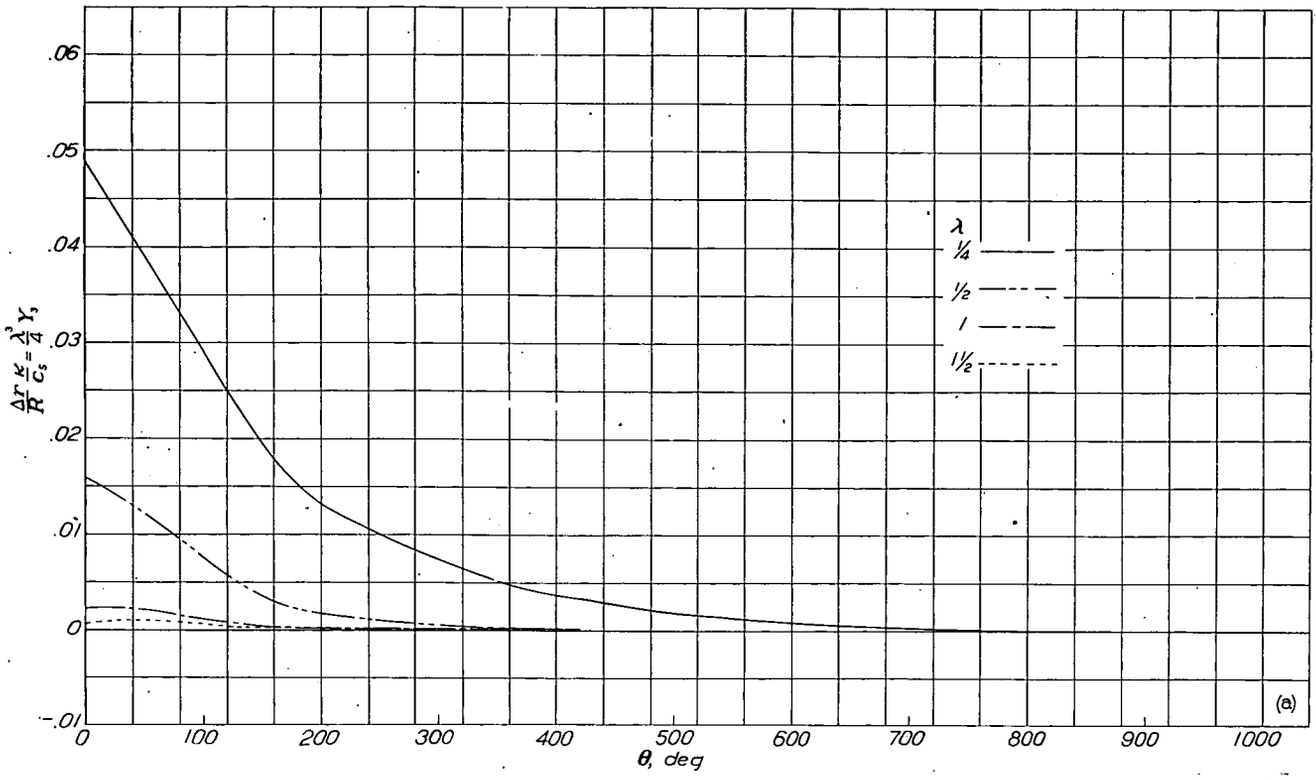

(a) Two-blade propeller. (See table V.)

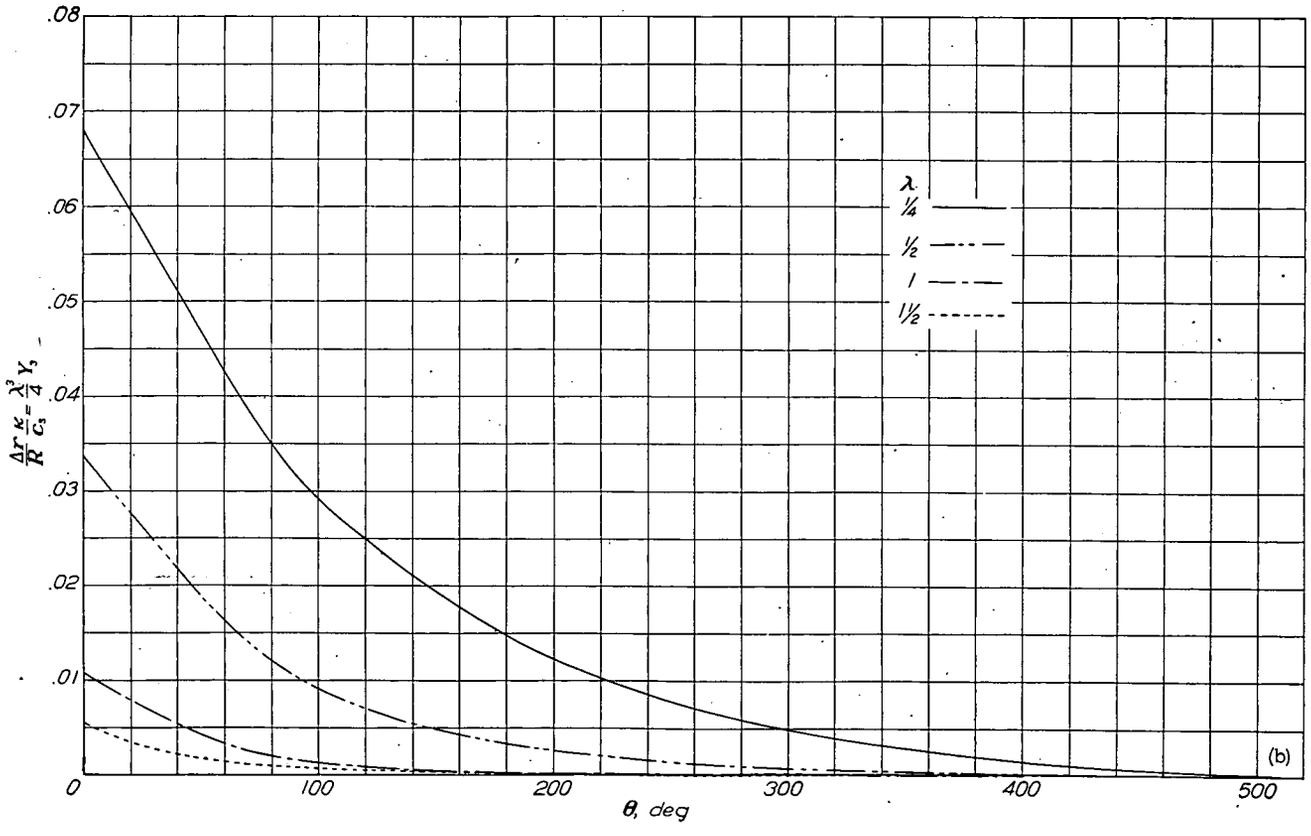

(b) Four-blade propeller. (See table VI.)

FIGURE 9.—The contour function $\frac{\Delta r}{R}\frac{\kappa}{c_i}=\frac{\lambda^3}{4}Y_3$ against θ for four values of λ.

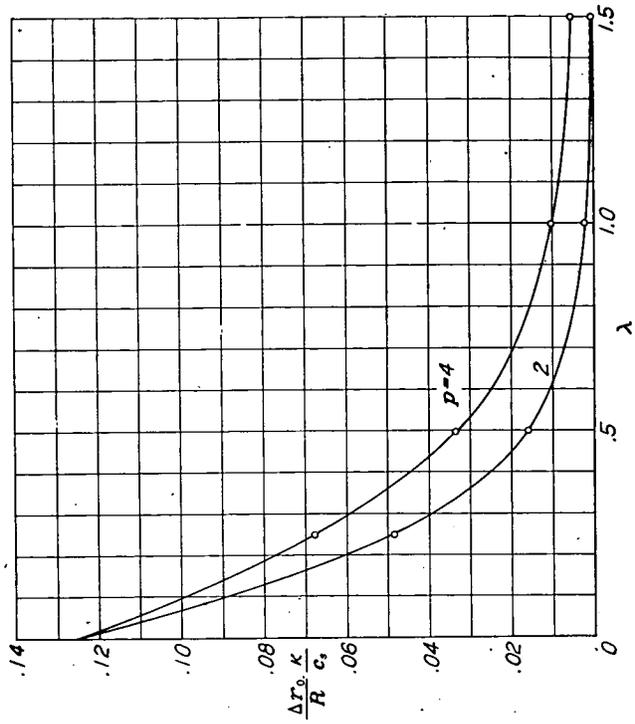

FIGURE 10.—Contraction coefficient $\frac{\Delta r_0}{R}\frac{\kappa}{c_1}$ against λ for two- and four-blade propellers.

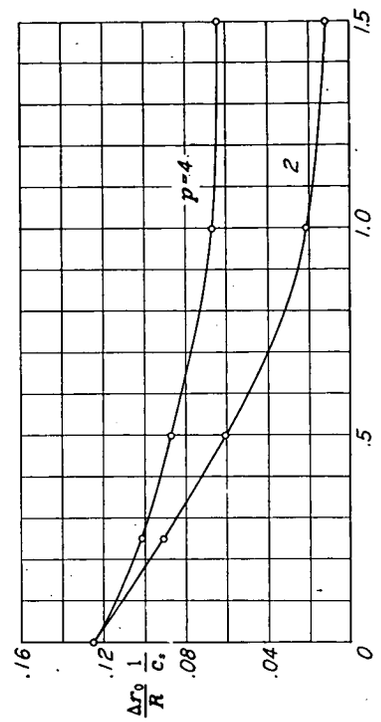

FIGURE 11.—Contraction coefficient $\frac{\Delta r_0}{R}\frac{1}{c_1}$ against λ for two- and, four-blade propellers.

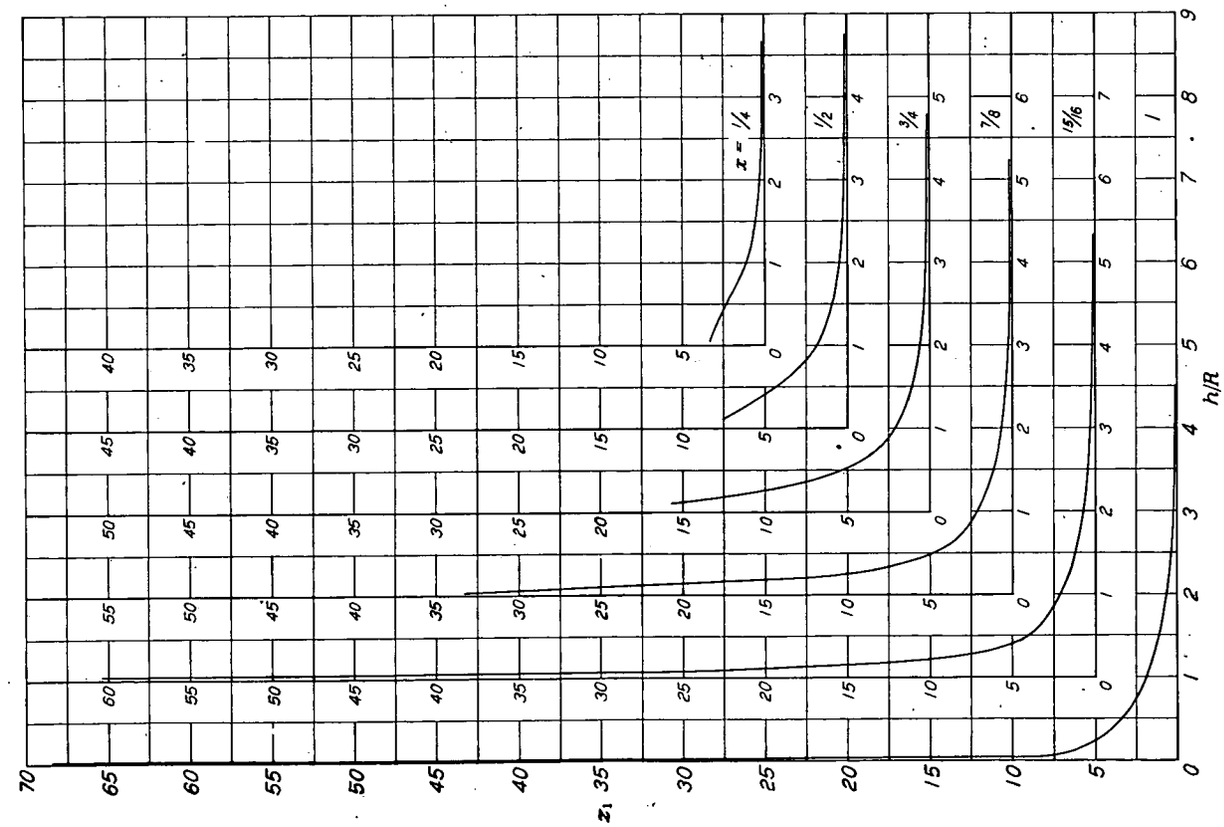

FIGURE 12.—The function z_1 against h/R for several values of x.

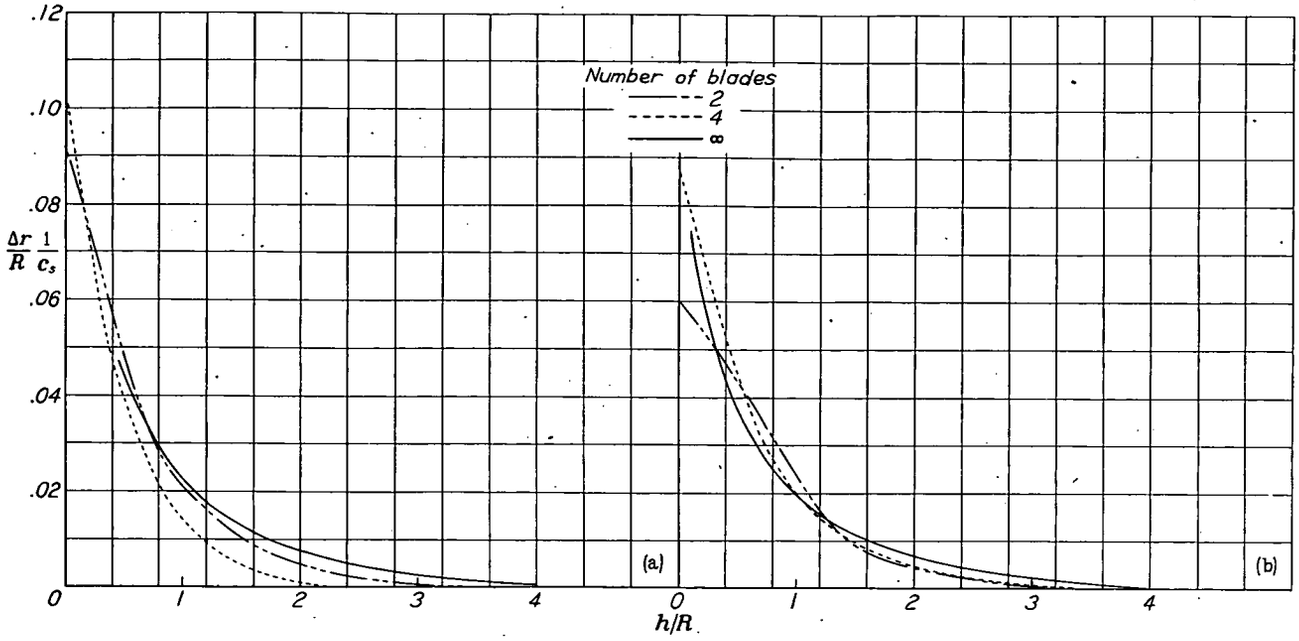

(a) λ=¼. (b) λ=½.

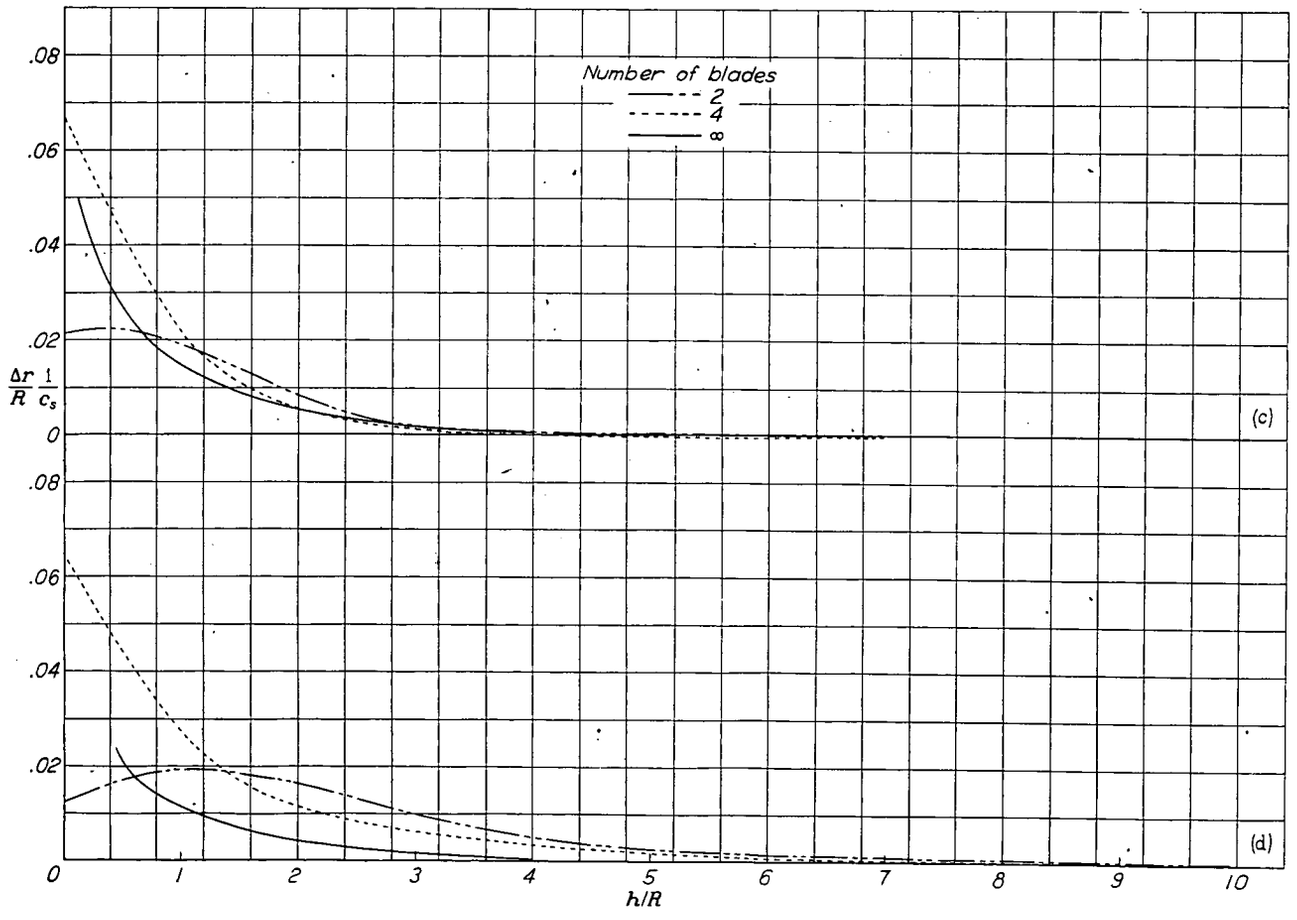

(c) λ=1. (d) λ=1½.

FIGURE 13.—Contour lines of wake helixes. (See table VII.)

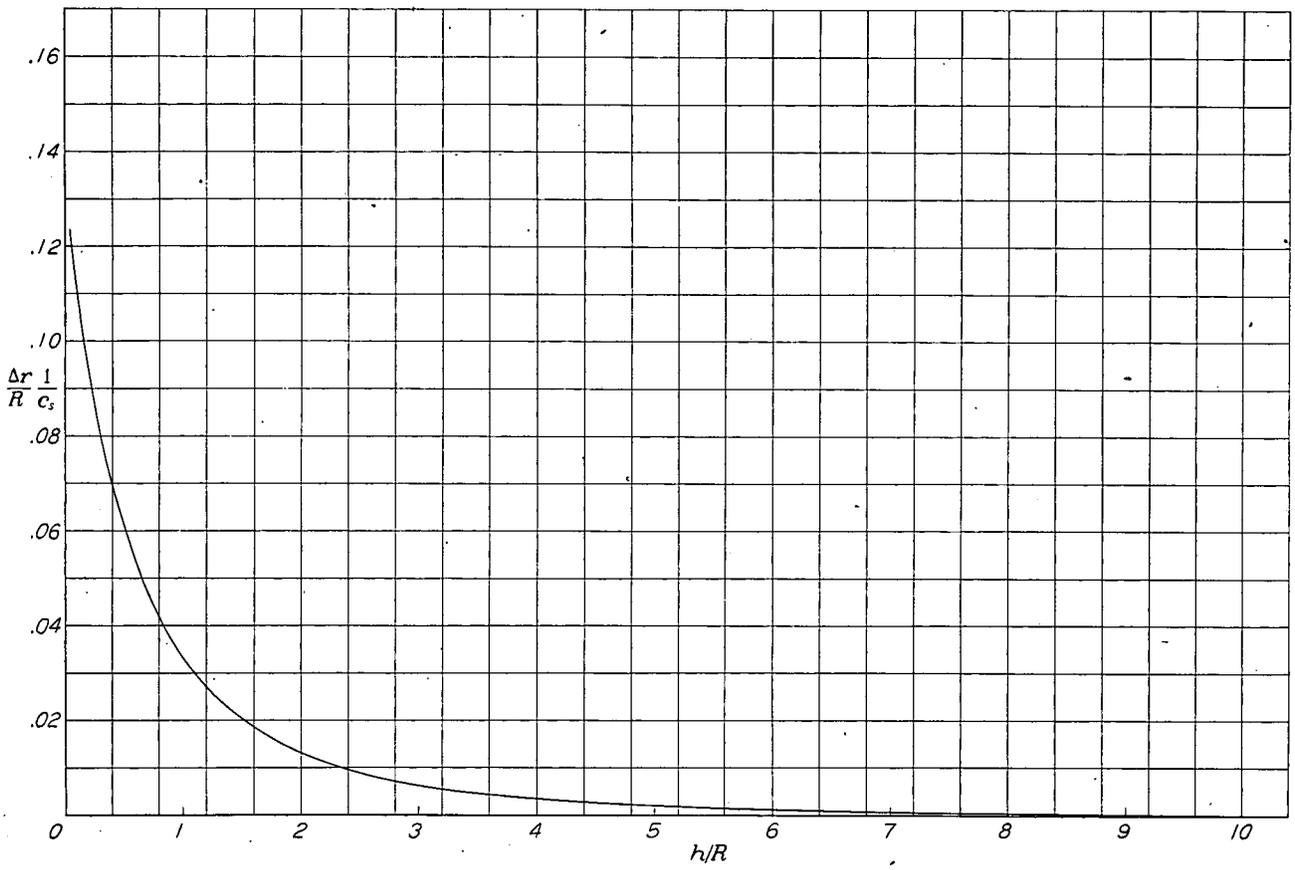

FIGURE 14.—Contour lines of wake for $p=\infty$. Dual rotation. (See table VIII.)

U. S. GOVERNMENT PRINTING OFFICE: 1947

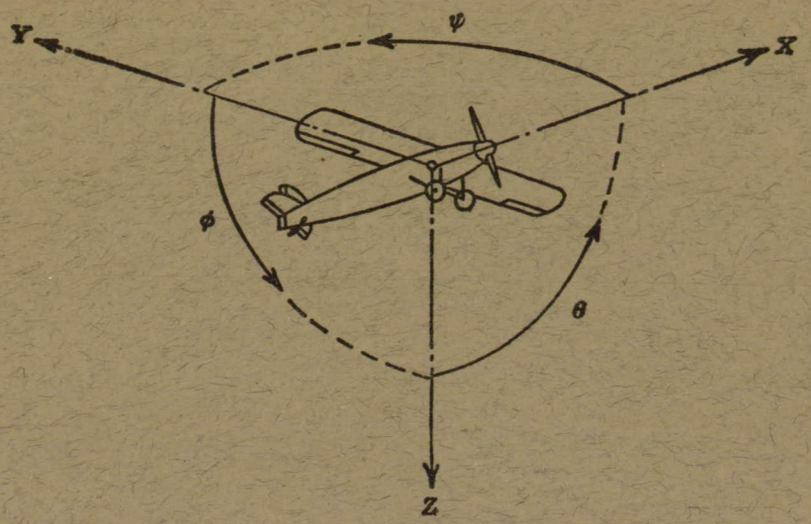

Positive directions of axes and angles (forces and moments) are shown by arrows

Axis		Force (parallel to axis) symbol	Moment about axis			Angle		Velocities	
Designation	Symbol		Designation	Symbol	Positive direction	Designation	Symbol	Linear (component along axis)	Angular
Longitudinal	X	X	Rolling	L	$Y \longrightarrow Z$	Roll	φ	u	p
Lateral	Y	Y	Pitching	M	$Z \longrightarrow X$	Pitch	θ	v	q
Normal	Z	Z	Yawing	N	$X \longrightarrow Y$	Yaw	ψ	w	r

Absolute coefficients of moment

$C_l = \frac{L}{qbS}$ (rolling) $\quad C_m = \frac{M}{qcS}$ (pitching) $\quad C_n = \frac{N}{qbS}$ (yawing)

Angle of set of control surface (relative to neutral position), δ. (Indicate surface by proper subscript.)

4. PROPELLER SYMBOLS

D Diameter

p Geometric pitch

p/D Pitch ratio

V' Inflow velocity

V_s Slipstream velocity

T Thrust, absolute coefficient $C_T = \frac{T}{\rho n^2 D^4}$

Q Torque, absolute coefficient $C_Q = \frac{Q}{\rho n^2 D^5}$

P Power, absolute coefficient $C_P = \frac{P}{\rho n^3 D^5}$

C_s Speed-power coefficient $= \sqrt[5]{\frac{\rho V^5}{P n^2}}$

η Efficiency

n Revolutions per second, rps

Φ Effective helix angle $= \tan^{-1}\left(\frac{V}{2\pi r n}\right)$

5. NUMERICAL RELATIONS

1 hp=76.04 kg-m/s=550 ft-lb/sec

1 metric horsepower=0.9863 hp

1 mph=0.4470 mps

1 mps=2.2369 mph

1 lb=0.4536 kg

1 kg=2.2046 lb

1 mi=1,609.35 m=5,280 ft

1 m=3.2808 ft